AD-A108 085 PACIFICA TECHNOLOGY DEL MAR CA F/G 13/13
IMPLEMENTATION OF ANISOTROPIC AND NONLINEAR THERMAL STRESS MODE--ETC(U)
AUG 81 R S DUNHAM, D E RANTA N00173-80-C-0385
UNCLASSIFIED PT-U81-0489-REV-1 NL

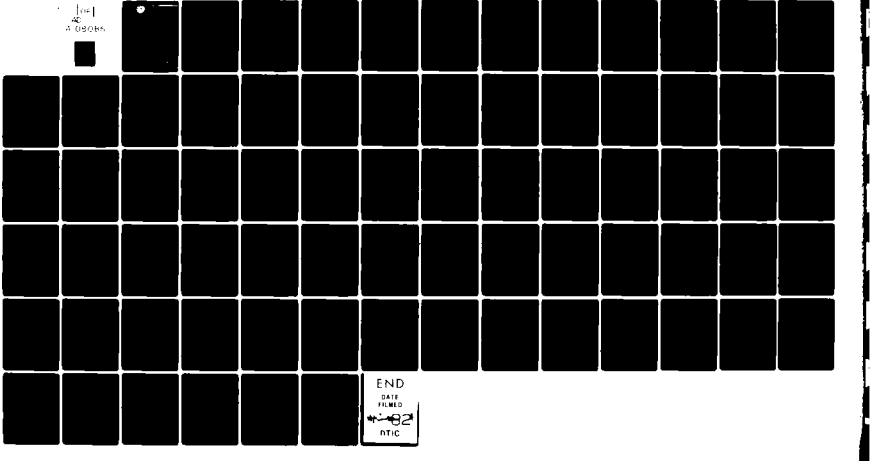

END
DATE FILMED
1-82
DTIC

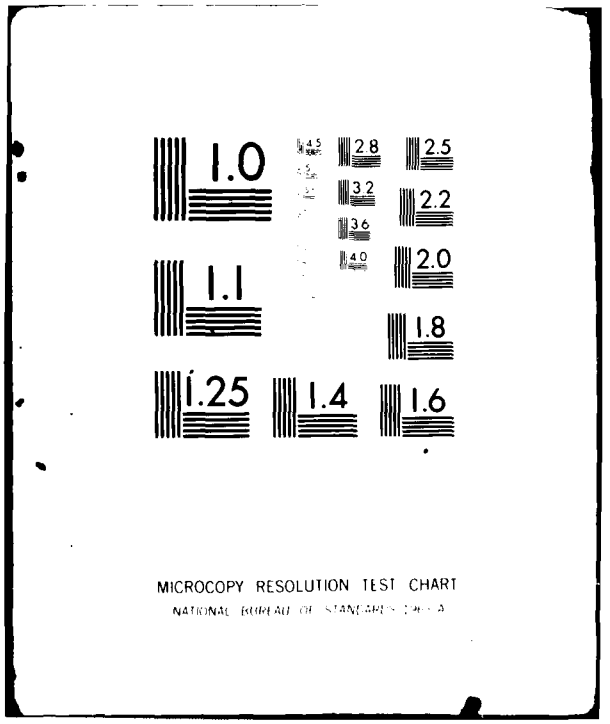
1.0
1.1
1.25
1.4
1.6
1.8
2.0
2.2
2.5
2.8
3.2
3.6
4.0
4.5
MICROCOPY RESOLUTION TEST CHART
NATIONAL BUREAU OF STANDARDS-1963-A

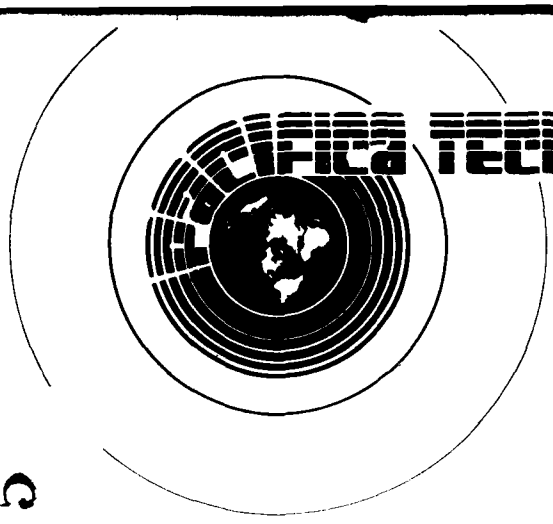

PT-U81-0489
(Revision 1)

FINAL REPORT

on

IMPLEMENTATION OF ANISOTROPIC AND NONLINEAR THERMAL STRESS MODELS IN ADINA 78

to the

U. S. Naval Research Laboratory
Washington, D. C.

by

Robert S. Dunham
and
Dale E. Ranta

August 1981

Corporate Office: 11696 Sorrento Valley Road, San Diego, CA 92121 P.O. Box 148, Del Mar, CA 92014 (714) 453-2530
Washington Office: 1710 Goodridge Drive, Suite 1318, McLean, VA 22102 (703) 734-8998

UNCLASSIFIED

SECURITY CLASSIFICATION OF THIS PAGE (When Data Entered)

REPORT DOCUMENTATION PAGE	READ INSTRUCTIONS BEFORE COMPLETING FORM
1. REPORT NUMBER	2. GOVT ACCESSION NO. AD-A108 085	3. RECIPIENT'S CATALOG NUMBER
4. TITLE (and Subtitle) Implementation of Anisotropic and Nonlinear Thermal Stress Models in ADINA 78	5. TYPE OF REPORT & PERIOD COVERED Final Report Aug 80 - Feb 81
	6. PERFORMING ORG. REPORT NUMBER PT-U81-0489, Rev.1
7. AUTHOR(s) Robert S. Dunham, Dale E. Ranta	8. CONTRACT OR GRANT NUMBER(s) N00173-80-C-0385
9. PERFORMING ORGANIZATION NAME AND ADDRESS Pacifica Technology P. O. Box 148 Del Mar, California 92014	10. PROGRAM ELEMENT, PROJECT, TASK AREA & WORK UNIT NUMBERS
11. CONTROLLING OFFICE NAME AND ADDRESS U. S. Naval Research Laboratory Washington, D. C. 20375	12. REPORT DATE August 1981
	13. NUMBER OF PAGES 70
14. MONITORING AGENCY NAME & ADDRESS(if different from Controlling Office)	15. SECURITY CLASS. (of this report) UNCLASSIFIED
	15a. DECLASSIFICATION/DOWNGRADING SCHEDULE NA
16. DISTRIBUTION STATEMENT (of this Report)	
17. DISTRIBUTION STATEMENT (of the abstract entered in Block 20, if different from Report)	
18. SUPPLEMENTARY NOTES	
19. KEY WORDS (Continue on reverse side if necessary and identify by block number) ADINA 78, Temperature Dependent Thermoelastic Anisotropic Model 12, Strain and Temperature Dependent Thermoelastic Anisotropic Model 6	

20. ABSTRACT (Continue on reverse side if necessary and identify by block number)

This report describes the improvements made to the ADINA 78 finite element computer code in order to permit the solution of structural response problems involving very rapid heating. A material model was added to the two- and three-dimensional continuum element types which permits the modeling of temperature dependent thermoelastic anisotropic material properties. A different material model was also added for these same continuum element types which permits the modeling of strain and temperature dependent thermoelastic anisotropic material properties. A major goal of this work was to render ADINA 78 operational on the

DD FORM 1 JAN 73 1473 EDITION OF 1 NOV 65 IS OBSOLETE

S/N 0102-LF-014-6601

UNCLASSIFIED

SECURITY CLASSIFICATION OF THIS PAGE (When Data Entered)

ASC computer at the Naval Research Laboratories as well as to improve the computational efficiency of the code by vectorizing the most important loops. This work and various benchmark test cases are also described.

ABSTRACT

This report describes the improvements made to the ADINA 78 finite element computer code in order to permit the solution of structural response problems involving very rapid heating. A material model was added to the two- and three-dimensional continuum element types which permits the modeling of temperature dependent thermoelastic anisotropic material properties. A different material model was also added for these same continuum element types which permits the modeling of strain and temperature dependent thermoelastic anisotropic material properties. A major goal of this work was to render ADINA 78 operational on the ASC computer at the Naval Research Laboratories as well as to improve the computational efficiency of the code by vectorizing the most important loops. This work and various benchmark test cases are also described.

ACKNOWLEDGEMENTS

The work described in this report was performed by personnel at Pacifica Technology in San Diego between August, 1980 and February, 1981 under Contract N00173-80-C-0385. The work was carried out under the guidance and supervision of Dr. C. L (Jim) Chang. His helpful guidance and cooperation are greatfully acknowledged. Chris Griffis provided valuable time saving information concerning ADINA and the ASC. His help is also gratefully acknowledged.

TABLE OF CONTENTS

TABLE OF CONTENTS

1. INTRODUCTION

For the past several years, personnel in the Materials Science and Technology Division of the Naval Research Laboratories (NRL) in Washington, D. C. have been actively engaged in research directed at understanding and predicting the effects of rapid heating of naval structural components. These efforts quickly focused on a small number of general purpose finite element computer programs that were capable of solving these problems. The ADINA[1,2] code was selected for these studies because it was the only general purpose code for which source coding was readily available at reasonable cost, and because the source coding was well written, modular, well documented and easy to modify for special applications. This report describes the improvements made to ADINA 78[3] in order to make it more suitable for the solution of structural response problems involving rapid heating.

The 1978 version of ADINA contained a material model (Model 3) for isotropic thermoelastic temperature dependent properties and a material model (Model 2) for anisotropic elastic properties for the two- and three-dimensional (2D & 3D) solid elements. However, there was no anisotropic thermoelastic temperature dependent model. This capability was added to ADINA 78 using Model 12 for the 2D & 3D solid element types. The implementation of this model, the necessary data cards together with sample problems are described in Section 2 of this report.

The main thermal problems of interest to NRL involve temperature excursions of hundreds of degrees (°F), consequently, the material response becomes nonlinear. In order to approximately model these thermal nonlinearities for anisotropic materials, Model 6 was also added to ADINA 78 for the 2D & 3D solid types. The implementation of this material model, the necessary data cards together with sample problems are described in Section 3 of this report.

Recently, the Naval Research Laboratory acquired a new and unique fourth generation, high speed digital computer, a Texas Instruments Advanced Scientific Computer (ASC). While the ASC is no longer in production and although there are only a few left in operation, it is a very powerful computer. The rated speed of the ASC for scalar operations is approximately equal to a CDC 6600 computer; additionally, the ASC has special hardware and software capabilities to perform "vector" floating point operations substantially faster than scalar operations. Prior to the current work, ADINA

had been run only in the scalar mode. Thus, a further facet of the current work was to "vectorize" ADINA to improve its computational efficiency on the ASC. This work and various benchmark test cases are described in Section 4.

Section 5 gives brief conclusions regarding the current effort and Section 6 contains recommendations for further improvements and modifications of ADINA.

Three appendices have been included to complete the report. Appendix A describes the ADINA files on the ASC, Appendix B briefly discusses various execution problems with ADINA, and Appendix C describes an Anisotropic Deformation Theory Plasticity that was considered for ADINA.

2. TEMPERATURE DEPENDENT ANISOTROPIC THERMOELASTIC MODEL

2.1 General

The 78 version of ADINA has available a large number of material models for 2D and 3D solid element types as indicated in Table 2.1.

Table 2.1 ADINA 78 Material Models for 2D & 3D Solid Element Types

NPAR(15) Model No.	Model Name
1	Isotropic Linear Elastic
2	Orthotropic (Anisotropic) Linear Elastic
3	Isotropic Thermoelastic
4	Curve Description
5	Concrete
7	Elastic-Plastic (Drucker-Prager-Cap)
8	Elastic-Plastic (von Mises, Isotropic Hardening)
9	Elastic-Plastic (Kinematic Hardening)
10	Thermoelastic-Plastic-Creep (von Mises, Isotropic Hardening)
11	Thermoelastic-Plastic-Creep (von Mises, Kinematic Hardening)
13	Incompressible Nonlinear Elastic (Mooney-Rivlin), 2D elements only

Unfortunately, ever since the original version of ADINA,[1,2] Bathe has retained this cumbersome identification of the material models. For example, while ADINA can model both orthotropic and thermoelastic problems via Model 2 and 3, respectively, it does not permit the modeling of orthotropic thermoelastic problems although the necessary coding for the calculation of the thermal force vector and local axes of material orthotrophy exist.

In order to properly model typical naval structures subjected to rapid, intense heating, it is necessary to have an anisotropic thermoelastic temperature dependent material model. Under the current effort this capability was added to ADINA 78 by implementing a new Model 12 as described in the remainder of this section.

In terms of compatibility with other ADINA options, Model 12 is identical to Model 3. It will work for dynamic or static, geometrically linear or nonlinear analyses, etc. However, Model 12 is intended for static, materially nonlinear analyses only. Its use with other options, while allowable as input to ADINA, may produce erroneous results. The user is encouraged to carefully verify use of Model 12 with these options. This was not done under the current effort.

Model 12 is very similar to Model 3 in the method used to store and retrieve material properties as a function of temperature from the PROP array (see Section 2.3). The strain and temperature dependent Model 6 described in Section 3 is likewise similar to Models 3 and 12. While Model 6 can be used without strain dependency to model temperature dependent anisotropic properties, this usage is not recommended; Model 12 is intended for these problems and is easier to use and more efficient.

2.2 Implementation of MODEL 12

Because ADINA was capable of treating isotropic thermoelastic materials and anisotropic materials, the implementation of Model 12 was straightforward, albeit nontrival. This section briefly describes the modifications and additions that were made to ADINA.

Logic was added in the element calling routine for the 2D (TODMFE) and 3D (THREDM) solid element types to establish storage boundaries for the new material property information that must be stored for Model 12. Logic was modified in the MATRT2 (2D) and MATWRT (3D) subroutines to read and print the new material property information. Minor changes were made to the 2D routines TDFE and QUADS in order to recalculate the orientation of the local material axes; no similar changes were needed for the 3D elements.

In the 2D and 3D solid element overlays there are subroutines present for each material model (1-13). Dummy subroutines EL2D12 and EL3D12 for Model 12 existed and these were replaced with functional logic that called the following suite of new subroutines that were added:

2D	3D
ITH212	ITH312
TH212	TH312
MROT2D	MROT3D

While the corrections were straightforward, they were nontrivial and fairly extensive in that approximately 1000 lines of code were added or modified.

2.3 Data Cards for MODEL 12

A small number of modifications to the ADINA 78 User's Manual[3] are necessary in order to describe how to use Model 12. However, there are no changes for any other material models. Rather than reproducing extensive portions of the user's manual, in the sequel only the modifications and additions to the manual are described.

The input requirements for Model 12 are essentially the same as for the hypothetical union of Models 2 and 3 and they follow the same format; they could be deduced from the existing manual by a clever user. The one difference is actually an improvement designed to eliminate needless input; M=NPAR(14) on the Element Group Control card has been used to define the number of temperatures at which the user wants to input different properties. At least 2 discrete temperatures should always be given ($M \geq 2$). There is no practical upper limit on M.

The material properties are stored in a table in a manner similar to the three-dimensional array PROP described on the succeeding pages. During the solution phase, the properties are linearly interpolated from the table as needed as illustrated in Figure 2-1. The temperatures must be given in strict, discrete, ascending order ($T_1 < T_2 < \ldots < T_m$); no two can be the same. Note that the properties are taken as undefined outside the given temperature range and execution is terminated if $T_1 > T > T_m$. The strain-stress law and its inverse the stress-strain compliance law are shown in Figures 2-2 and 2-3, respectively. For Model 12 the interpolation is performed on the stress-strain compliances given in Figure 2-3 and not on the moduli, Poisson's ratio and coefficients of thermal expansion.

In order to avoid needless duplication within this report, the following description combines the data cards for the 2D (Section XII of the ADINA 78 User's Manual[3] pages

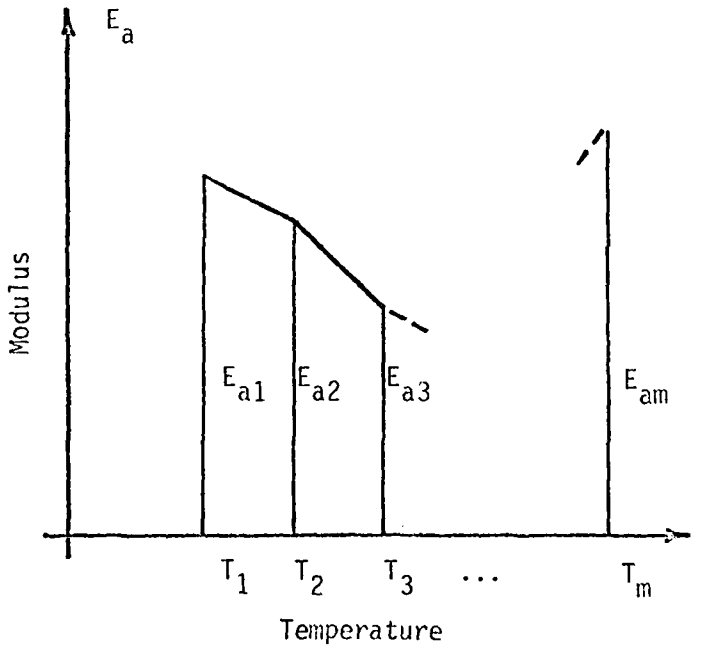

Figure 2-1. Model 12 (and 6) Temperature Interpolation Method.

$$\begin{Bmatrix} \varepsilon_a - \alpha_a \Delta T \\ \varepsilon_b - \alpha_b \Delta T \\ \varepsilon_c - \alpha_c \Delta T \\ \gamma_{ab} \\ \gamma_{ac} \\ \gamma_{bc} \end{Bmatrix} = \begin{bmatrix} 1/E_a & -\nu_{ab}/E_b & -\nu_{ac}/E_c & 0 & 0 & 0 \\ -\nu_{ba}/E_a & 1/E_b & -\nu_{bc}/E_c & 0 & 0 & 0 \\ -\nu_{ca}/E_a & -\nu_{cb}/E_b & 1/E_c & 0 & 0 & 0 \\ 0 & 0 & 0 & 1/G_{ab} & 0 & 0 \\ 0 & 0 & 0 & 0 & 1/G_{ac} & 0 \\ 0 & 0 & 0 & 0 & 0 & 1/G_{bc} \end{bmatrix} \begin{Bmatrix} \sigma_a \\ \sigma_b \\ \sigma_c \\ \sigma_{ab} \\ \sigma_{ac} \\ \sigma_{bc} \end{Bmatrix}$$

where the ε_i and σ_i are the normal strains and stresses in the x_i directions, and γ_{ij} and σ_{ij} are the corresponding engineering shear strains and shear stresses,respectively, and ΔT is the temperature above the stress free refrence temperature, $\Delta T = T\text{-}TREF$.

Note $\nu_{ba}/E_a = \nu_{ab}/E_b$, etc.

Figure 2-2 Strain-Stress Law for MODELS 3 and 12.

$$\begin{Bmatrix} \sigma_a \\ \sigma_b \\ \sigma_c \\ \sigma_{ab} \\ \sigma_{ac} \\ \sigma_{bc} \end{Bmatrix} = \begin{bmatrix} C_{aa} & C_{ab} & C_{ac} & 0 & 0 & 0 \\ C_{ab} & C_{bb} & C_{bc} & 0 & 0 & 0 \\ C_{ac} & C_{bc} & C_{cc} & 0 & 0 & 0 \\ 0 & 0 & 0 & G_{ab} & 0 & 0 \\ 0 & 0 & 0 & 0 & G_{ac} & 0 \\ 0 & 0 & 0 & 0 & 0 & G_{bc} \end{bmatrix} \begin{Bmatrix} \varepsilon_a - \alpha_a \Delta T \\ \varepsilon_b - \alpha_b \Delta T \\ \varepsilon_c - \alpha_c \Delta T \\ \gamma_{ab} \\ \gamma_{ac} \\ \gamma_{bc} \end{Bmatrix}$$

Figure 2-3 Stress-Strain Compliances for MODELS 3 and 12.

4 - 17) and 3D (Section XIII of the manual, pages 4 - 17) solid element types.

Modifications for the 2D and 3D Solid Element Input Data (MODEL 12)

Element Group Control Card (2014)

Columns	Variable	Entry
•		
•		
•		
53-56	M=NPAR(14)	Number of temperature points (Models 6&12 only)
57-60	NPAR(15)=12	Material model number; 12 is the Orthotropic Thermoelastic Model number
•		
•		
•		

Set NPAR(15) = 12 to activate material Model 12 input data. M = NPAR(14)>2 must also be set for material Model 12. Otherwise, the Element Group Control Card data is unchanged.

Material MODEL 12 Property Data Cards

Each of the following card sets must have at least 1 card with 2 temperature points (M ≥ 2). If M > 8, use as many cards as needed in format 8F10.0. The 2D and 3D solid material model 12 requires, respectively, 10 and 12 card sets corresponding to the following properties: E_a; E_b; E_c; ν_{ab}; ν_{ac}; ν_{bc}; G_{ab}; G_{ac}*; G_{bc}*; α_a; α_b; and α_c. The subscripts a,b,c refer to the local orthogonal principal material axes as defined in Section XII and XIII, respectively, for 2D and 3D solids. For 2D solids, the a-b axes lie in the y-z plane of modeling. Note that while the stress-strain law is orthotropic in the local (a,b,c) material coordinate system (Figure 2-3), it is "anisotropic" in the global coordinate

*Note that G_{ac} and G_{bc} are not defined for 2D solids; thus, card sets 8 and 9 are omitted for 2D solid elements.

system. A local anisotropic model could easily be added at the expense of 4 additional data sets for 2D and 15 additional sets for 3D solids. The following describes the material property data cards read for Model 12.

Columns	Variable	Entry
Card Set 1		
1 - 10	PROP(1,N,1)	T_1 temperature at point 1
11 - 20	PROP(2,N,1)	T_2 temperature at point 2
.	.	.
.	.	.
.	.	.
	PROP(M,N,1)	T_m temperature at point m
Card Set 2		
1 - 10	PROP(1,N,2)	E_{a1} a-direction modulus at point 1
11 - 20	PROP(2,N,2)	E_{a2} a-direction modulus at point 2
.	.	.
.	.	.
.	.	.
	PROP(M,N,2)	E_{am} a-direction modulus at point m
Card Set 3		
1 - 10	PROP(1,N,3)	E_{b1} b-direction modulus at point 1
11 - 20	PROP(2,N,3)	E_{b2} b-direction modulus at point 2
.	.	.
.	.	.
.	.	.
	PROP(M,N,3)	E_{bm} b-direction modulus at point m
Card Set 4		
1 - 10	PROP(1,N,4)	E_{c1} c-direction modulus at point 1
11 - 20	PROP(2,N,4)	E_{c2} c-direction modulus at point 2
.	.	.
.	.	.
.	.	.
	PROP(M,N,4)	E_{cm} c-direction modulus at point m
Card Set 5		
1 - 10	PROP(1,N,5)	ν_{ab1} ab-Poisson's ratio at point 1
11 - 20	PROP(2,N,5)	ν_{ab2} ab-Poisson's ratio at point 2
.	.	.
.	.	.
.	.	.
	PROP(M,N,5)	ν_{abm} ab-Poisson's ratio at point m

Card Set 6

1 - 10	PROP(1,N,6)	ν_{ac1} ac-Poisson's ratio at point 1
11 - 20	PROP(2,N,6)	ν_{ac2} ac-Poisson's ratio at point 2
.	.	.
.	.	.
.	.	.
	PROP(M,N,6)	ν_{acm} ac-Poisson's ratio at point m

Card Set 7

1 - 10	PROP(1,N,7)	ν_{bc1} bc-Poisson's ratio at point 1
11 - 20	PROP(2,N,7)	ν_{bc2} bc-Poisson's ratio at point 2
.	.	.
.	.	.
.	.	.
	PROP(M,N,7)	ν_{bcm} bc-Poisson's ratio at point m

Card Set 8*

1 - 10	PROP(1,N,8)	G_{ab1} ab-shear modulus at point 1
11 - 20	PROP(2,N,8)	G_{ab2} ab-shear modulus at point 2
.	.	.
.	.	.
.	.	.
	PROP(M,N,8)	G_{abm} ab-shear modulus at point m

Card Set 9*

1 - 10	PROP(1,N,9)	G_{ac1} ac-shear modulus at point 1
11 - 20	PROP(2,N,9)	G_{ac2} ac-shear modulus at point 2
.	.	.
.	.	.
.	.	.
	PROP(M,N,9)	G_{acm} ac-shear modulus at point m

Card Set 10

1 - 10	PROP(1,N,10)	G_{bc1} bc-shear modulus at point 1
11 - 20	PROP(2,N,10)	G_{bc2} bc-shear modulus at point 2
.	.	.
.	.	.
.	.	.
	PROP(M,N,10)	G_{bcm} bc-shear modulus at point m

Card Set 11

1 - 10	PROP(1,N,11)	α_{a1} a-direction expansion coefficient at point 1
11 - 20	PROP(2,N,11)	α_{a2} a-direction expansion coefficient at point 2
.	.	.
.	.	.
.	.	.
	PROP(M,N,11)	α_{am} a-direction expansion coefficient at point m

*Card Sets 8 & 9 must be omitted for two-dimensional problems.

Card Set 12

1 - 10	PROP(1,N,12)	α_{b1} b-direction expansion coefficient at point 1
11 - 20	PROP(2,N,12)	α_{b2} b-direction expansion coefficient at point 2
.	.	.
.	.	.
.	.	.
	PROP(M,N,12)	α_{bm} b-direction expansion coefficient at point m

Card Set 13

1 - 10	PROP(1,N,13)	α_{c1} c-direction expansion coefficient at point 1
11 - 20	PROP(2,N,13)	α_{c2} c-direction expansion coefficient at point 2
.	.	
.	.	.
.	.	.
	PROP(M,N,13)	α_{cm} c-direction expansion coefficient at point m

Card Set 14

1 - 10	PROP(1,N,14)	TREF reference stress free temperature

2.4 Sample Problems for MODEL 12

A two-dimensional and similar three-dimensional sample problem was run to validate the new Model 12 logic added to ADINA 78. Figures 2-4 and 2-5 show the 2D and 3D problem geometries, respectively. The 2D problem is a plane strain 90° segment of a thin axisymmetric ring. The mean radius of the ring is 20" and the thickness is 0.5".

Symmetry boundary conditions are applied on the y-(u_z=0) and z-(u_y=0) axes, so that the solution is symmetric about the x-axis. A total of nine 8-node, bi-quadratic quadrilateral elements spaced at 10° and 46 nodal points were used as shown in Figure 2-4. The loading consisted of a 333 psi external pressure and the thermal loading described below.

Temperature dependent orthotropic moduli and orthotropic thermal expansion coefficients were used as shown in Figures 2-6a & b. The stress free reference temperature was TREF = 0 and the temperature at which the calculation was done was T = 10. Thus, from Figures 2-6a & b

$E_a = 1 \times 10^6$ psi
$E_b = 1.5 \times 10^6$ psi
$E_c = 2 \times 10^6$ psi
$G_{ab} = .1 \times 10^6$ psi
$\alpha_a = .01$, $\alpha_a \Delta T = .1$
$\alpha_b = .02$, $\alpha_b \Delta T = .2$
$\alpha_c = .03$, $\alpha_c \Delta T = .3$

Poisson's ratios were taken to be temperature independent, however, they were orthotropic

$\nu_{ab} = .1$
$\nu_{ac} = .2$
$\nu_{bc} = .3$

The ADINA 78 data cards are given in Tables 2.2 and 2.3 for the 2D and 3D problems, respectively. The 2D Model 12 problem corresponds to the file R2D3 in Appendix A and the 3D problem to file R3D2. The solutions to the 2D and 3D problems are identical (in closed form, not numerically) and are as follows

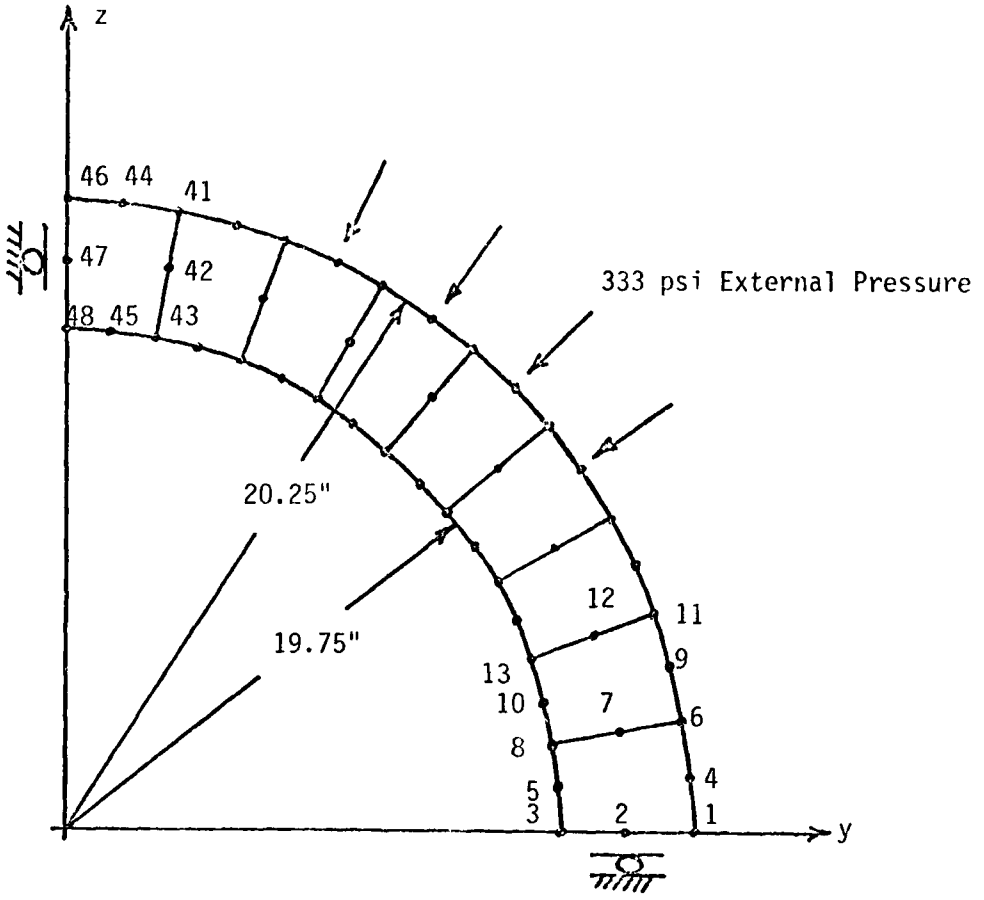

Figure 2-4. 2D Model 12 Sample Problem - File R2D3 Appendix A.

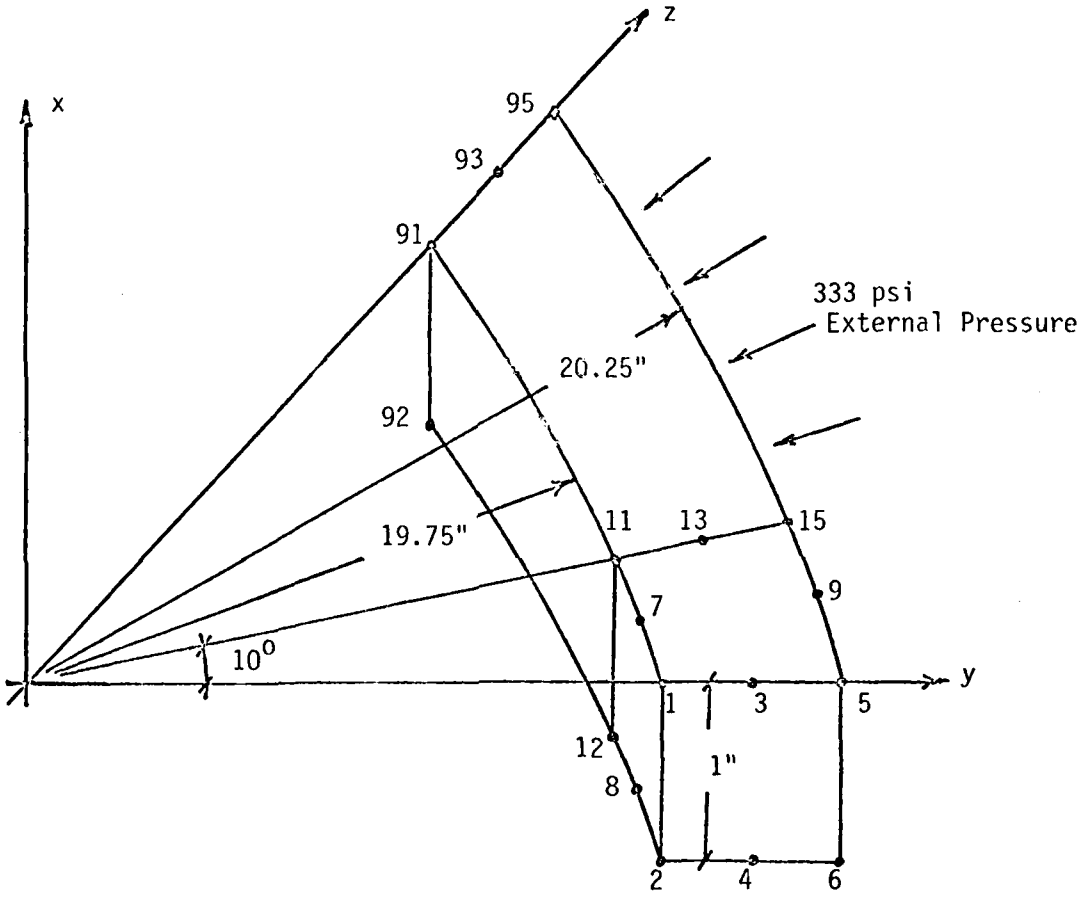

Figure 2-5. 3D Model 12 Sample Problem - File R3D2 Appendix A.

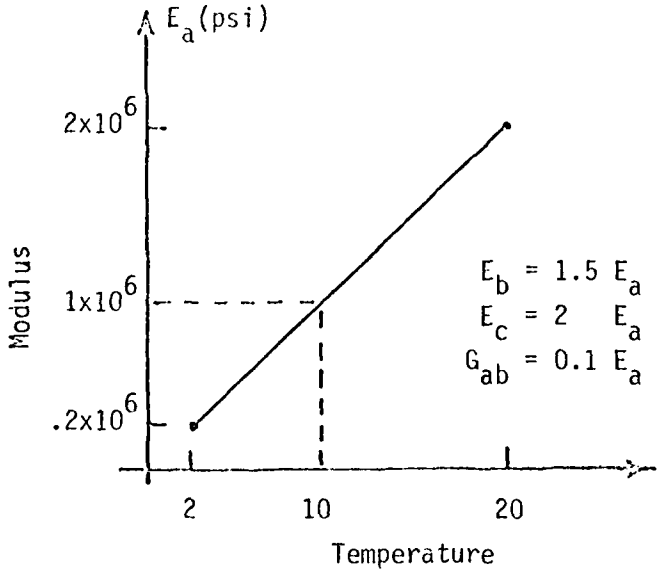

Figure 2-6a. Temperature Dependent Modulus

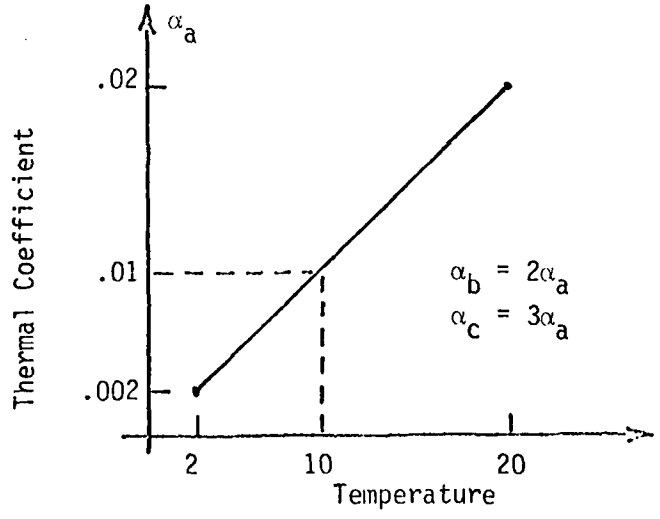

Figure 2-6b. Temperature Dependent Thermal Coefficient.

```
2-D HOOP MODEL 12
   48100111          1     1     1          1.                    1
         2
         9                                  2

     2    2
     1    2
          0.          0.          10.          10.
     2    2
          0.          10.         10.          10.
X    1    1     0     1     1     1     1                  20.25
X    4    1     0     0     1     1     1                  20.25          5.     5
X   44    1     0     0     1     1     1                  20.25         85.
X    6    1     0     0     1     1     1                  20.25         10.     5
X   46    1     1     0     1     1     1                  20.25         90.
X    2    1     0     1     1     1     1                  20.00
X    7    1     0     0     1     1     1                  20.00         10.     5
X   47    1     1     0     1     1     1                  20.00         90.
X    3    1     0     1     1     1     1                  19.75
X    5    1     0     0     1     1     1                  19.75          5.     5
X   45    1     0     0     1     1     1                  19.75         85.
X    8    1     0     0     1     1     1                  19.75         10.     5
X   48    1     1     0     1     1     1                  19.75         90.
                  1     1
     1          10.     1
    48          10.
    2   9   1          1                                        2  12
     1
          2.          20.
        2.0E5       2.0E6
        3.0E5       3.0E6
        4.0E5       4.0E6
           .1          .1
           .2          .2
           .3          .3
        2.0E4       2.0E5
         .002          .02
         .004          .04
         .006          .06
           0.
     1     8     1     1     5       .087266463          1.0
     3     1     6     8     2     4     7     5
     9     8     1     1     5       .087266463          1.0
    43    41    46    48    42    44    47    45
     2     1     1     6     4
333.333333 333.33333          1.0                  5
     2     1    41    46    44
333.333333 333.33333          1.
     1     2          1.                  1
    48     2          1.
STOP
```

Table 2.2. 2D Solid Element Model 12 Sample Problem - File R2D3 Appendix A.

```
HOOP STRAIN  -  3D     PLANE STRAIN  MODEL 12
   97100111          1     1     1        1.                 1
         2
               9                      2








    2     2
    1     2
         0.        1.        10.        1.
    2     2
         0.       10.        10.       10.
X   1     0     0     1     1     1     1                19.75
X   7     0     0     0     1     1     1                19.75        5.     10
X  87     0     0     0     1     1     1                19.75       85.
X  11     0     0     0     1     1     1                19.75       10.     10
X  91     0     1     0     1     1     1                19.75       90.
X   3     0     0     1     1     1     1                20.00
X  13     0     0     0     1     1     1                20.00       10.     10
X  93     0     1     0     1     1     1                20.00       90.
X   5     0     0     1     1     1     1                20.25
X   9     0     0     0     1     1     1                20.25        5.     10
X  89     0     0     0     1     1     1                20.25       85.
X  15     0     0     0     1     1     1                20.25       10.     10
X  95     0     1     0     1     1     1                20.25       90.
X   2     1     0     1     1     1     1       -1.0     19.75
X   8     1     0     0     1     1     1       -1.0     19.75        5.     10
X  88     1     0     0     1     1     1       -1.0     19.75       85.
X  12     1     0     0     1     1     1       -1.0     19.75       10.     10
X  92     1     1     0     1     1     1       -1.0     19.75       90.
X   4     1     0     1     1     1     1       -1.0     20.00
X  14     1     0     0     1     1     1       -1.0     20.00       10.     10
X  94     1     1     0     1     1     1       -1.0     20.00       90.
X   6     1     0     1     1     1     1       -1.0     20.25
X  10     1     0     0     1     1     1       -1.0     20.25        5.     10
X  90     1     0     0     1     1     1       -1.0     20.25       85.
X  16     1     0     0     1     1     1       -1.0     20.25       10.     10
X  96     1     1     0     1     1     1       -1.0     20.25       90.
   97     1     1     1     1     1     1
                1     1
    1        10.      1
   97        10.
   3    9    1               16                            2   12          9
    1
         2.        20.
     2.0E5      2.0E6
     3.0E5      3.0E6
     4.0E5      4.0E6
        .1         .1
        .2         .2
        .3         .3
     2.0E4      2.0E5
     3.0E4      3.0E5
     6.0E4      6.0E5
      .002        .02
      .004        .04
      .006        .06
        0.
```

Table 2.3. 3D Solid Element Model 12 Sample Problem - File R3D2 Appendix A.

```
     1    97     7    95
     1    97    17    95
     1    97    27    95
     1    97    37    95
     1    97    47    95
     1    97    57    95
     1    97    67    95
     1    97    77    95
     1    97    87    95
     1    16    16     1     1     1          10
    16    15     5     6    12    11     1     2
     0     9     0    10     0     7     0     8    14    13     3     4     0
     2    16    16     1     1     2          10
    26    25    15    16    22    21    11    12
     0    19     0    20     0    17     0    18    24    23    13    14     0
     3    16    16     1     1     3          10
    36    35    25    26    32    31    21    22
     0    29     0    30     0    27     0    28    34    33    23    24     0
     4    16    16     1     1     4          10
    46    45    35    36    42    41    31    32
     0    39     0    40     0    37     0    38    44    43    33    34     0
     5    16    16     1     1     5          10
    56    55    45    46    52    51    41    42
     0    49     0    50     0    47     0    48    54    53    43    44     0
     6    16    16     1     1     6          10
    66    65    55    56    62    61    51    52
     0    59     0    60     0    57     0    58    64    63    53    54     0
     7    16    16     1     1     7          10
    76    75    65    66    72    71    61    62
     0    69     0    70     0    67     0    68    74    73    63    64     0
     8    16    16     1     1     8          10
    86    85    75    76    82    81    71    72
     0    79     0    80     0    77     0    78    84    83    73    74     0
     9    16    16     1     1     9          10
    96    95    85    86    92    91    81    82
     0    89     0    90     0    87     0    88    94    93    83    84     0
     1    16    15     5     6     0     9     0    10
333.3333  333.3333  333.3333  333.3333                    10
     1    96    95    85    86     0    89     0    90
333.3333  333.3333  333.3333  333.3333
     1     2          1.                  1
    97     2          1.
STOP
```

Table 2.3.(cont'd) 3D Solid Element Model 12 Sample Problem - File R3D2 Appendix A.

$$\tau_x = 0 \quad , \quad \sigma_r = 0$$

where r, the radial direction, corresponds to the ADINA a direction, x corresponds to the c direction and b to the θ or hoop direction. Note the 2D properties have been rotated 5° (.073 radians) so that a is in the radial direction at the center of the element. (The BET material angle listed on page XI.43 of the ADINA manual must be given in radians, not degrees as the manual specifies.) Likewise, the 3D material axes orientation cards rotate the properties so that the a direction is in the radial direction at the center of the element. Thus, the results are numerically symmetric about the x-axis. The strain-stress law becomes

$$\begin{Bmatrix} \varepsilon_r - .1 \\ \varepsilon_\theta - .2 \\ \varepsilon_x - .3 \end{Bmatrix} = \begin{bmatrix} 1 & -.1/1.5 & -.1 \\ -.1/1.5 & 1/1.5 & -.15 \\ -.1 & -.15 & .5 \end{bmatrix} \begin{Bmatrix} \sigma_r \\ \sigma_\theta \\ \sigma_x \end{Bmatrix} \times 10^{-6}$$

Because the ring is thin and free to expand, the hoop stress is

$$\sigma_\theta = - \frac{pR}{t} = -13333 \text{ psi}$$

Solving for the 3 remaining unknowns gives

$$\sigma_x = -606000 \text{ psi}$$

and

$$\varepsilon_r = .1615$$
$$\varepsilon_\theta = .2820$$

Thus the radial displacement is

$$u_r = R\,\varepsilon_\theta = 5.640$$

The numerical solutions given by ADINA agree closely with these values as shown in Tables 2.4 and 2.5

Table 2.4 Computed Nodal Point Displacements

	2D		3D	
Radius	Node	Displacement	Node	Displacement
19.75	3	5.597	1	5.597
20	2	5.639	3	5.639
20.25	1	5.680	5	5.680

Table 2.5 Computed Element Stresses

	2D		3D	
Output Pt. 2D/3D	σ_x	σ_θ	σ_x	σ_θ
1/2	-604504	-14581	-604504	-14835
3/1	-603653	-11917	-603653	-12128

3. TEMPERATURE DEPENDENT ANISOTROPIC THERMOELASTIC MODEL

3.1 General

Over a temperature range of several hundreds of degrees (°F), the materials used in important naval structures experience a significant level of strain. The mechanical properties of these same materials are altered as a function of the level of strain as well as a function of the temperature. The variation in mechanical properties as a function of temperature can be modeled in ADINA 78 as described in Section 2. However, there is still a need to model the variation in properties as a function of strain. This section describes the addition to ADINA 78 of material Model 6 that is capable of modeling the strain dependency and the combined strain and temperature dependency of the material properties.

Physically Nonlinear Elastic Materials

The dependency of the elastic constants on strain is a class of problems in mechanics known as physically nonlinear or nonlinear elasticity problems. This class distinction is independent of kinematic nonlinearities (large deformations or finite elasticity) and temperature dependency. It is an extremely complex class of problems that is not frequently found in the literature[4,5] and often is improperly treated (especially in soil mechanics). The proper invariant treatment of materials of this class requires the development of a constitutive equation of the form

$$\sigma_{ij} = \frac{\partial U}{\partial \varepsilon_{ij}}$$

where $U = U(I_1, I_2, I_3, A_k)$ is the strain energy density expressed as a function of the 3 invariants of the strain tensor

$$I_1 = \varepsilon_{ii}$$
$$I_2 = \varepsilon_{ij}\varepsilon_{ji}$$
$$I_3 = \varepsilon_{ij}\varepsilon_{jk}\varepsilon_{ki}$$

and the 3 vectors (A_k) describing the local principal material directions for anisotropic materials. Note that even if the strain energy density does not depend on A_k, the material is isotropic only about the undeformed state ($I_1=I_2=I_3=0$) and, in general, is highly anisotropic otherwise.

The strain energy density for isotropic, linear elastic materials is expressed

$$U = \mu \; I_1^2 \; + \; \frac{1}{2} \; \lambda \; I_2$$

where μ and λ are the Lame constants. Thus

$$\sigma_{ij} = 2\mu \; \varepsilon_{ij} \; + \; \lambda \varepsilon_{kk} \; \delta_{ij}$$

For a typical nonlinear elastic material, tests must be performed to measure the unknown "elastic" constants in a polynominal expansion of the strain energy density

$$U = A_{12} \; I_1^2 + A_{22} \; I_2 + A_{13} \; I_1^3 + A_{23} \; I_1 \; I_2 + A_{33} \; I_3 + A_{14} \; I_1^4 + A_{24} \; I_1^2 \; I_2 + A_{34} \; I_1 \; I_3 + A_{35} \; I_2^2 + \ldots +$$

For even the simpliest material this task becomes hopeless. There are so many constants that an almost infinite number of tests must be performed to determine their values. This type of approach has rarely been successful. (However, one exception is the Mooney-Rivlin rubber like material model available in ADINA.)

A more tractable approach is the deformation theory plasticity model described in Appendix C.[6] Deformation theory plasticity seeks to approximate nonlinear, path independent, stress-strain behavior for loading paths that experience no unloading. These theories have been successfully used to treat several anisotropic materials commonly used in naval structures.[6,7] Deformation theory requires the solution of only a path independent nonlinear elasticity problem, not a plasticity problem. ADINA has a nonlinear static solution procedure that uses a secant stiffness matrix that is very compatible with the deformation theory approach.

Implementation of the deformation theory plasticity model described in Appendix C in the ADINA code would have required a major effort well beyond the scope of the present work. Such an effort would be justified only if the theory were essential to

predicting the response of structural materials to rapid, intense treating. It was felt that this level of effort was not justified, and instead it was decided to implement a simplier model that would permit the user to describe the usual anisotropic elastic constants as a function of strain. While this model is not invariant, it can be used to approximately model mild nonlinearities in materials that undergo path independent loading only. The remainder of this section describes the material Model 6 that was implemented in ADINA to treat strain and temperature dependent properties.

3.2 Implementation of MODEL 6

The implementation of Model 6 was straightforward but nontrival and closely follows that of Model 12. The implementation of Model 6 was limited to the 2D and 3D solid elements and it is compatible with all of the other options in ADINA. However, the user is again warned that the present effort validated Model 6 only for the problems described herein.

Logic was modified in the MATRT2 (2D) and MATWRT (3D) subroutines to read and print the new material property information. In the 2D and 3D solid element overlays there are subroutines present for each material model (1-13). Dummy subroutines ELT2D6 and ELT3D6 for Model 6 existed and these were replaced with functional logic that called the following suite of new subroutines that were added:

2D	3D
ITH206	ITH306
TH206	TH306
MR206	M3D06
GM2D06	GM3D06

While the corrections were straightforward they were nontrivial and fairly extensive in that approximately 1000 lines of code were added or modified.

3.3 Data Cards for MODEL 6

Model 6 is very similar to Models 12 and 3 in the method used to store and

retrieve material properties from the array PROP as a function of strain and temperature. While Model 6 can be used without strain dependency to model temperature dependent anisotropic materials, this usage is inefficient and not recommended. Model 12 is intended for these problems and is easier to use. The material properties are stored in a table in a manner similar to the pseudo four-dimensional array PROP described on the succeeding pages. During the solution phase the properties are linearly interpolated as illustrated in Figures 3-1 and 2-1. Model 6 is biased in favor of strain dependency so this interpolation is performed first. If more than one temperature point is used (M=NPAR(14) > 1), then the temperature interpolation is performed on the strain interpolated properties. Strain and temperature points must be given in strict, discrete, ascending order ($\varepsilon_1<\varepsilon_2<\ldots<\varepsilon_k$ and $T_1<T_2\ldots<T_m$). Note that the properties are taken as undefined outside the specified strain and temperature range and execution is terminated if $\varepsilon_1 > \varepsilon > \varepsilon_k$ or $T_1 > T > T_m$. Note also that the strain range must include negative values for compression (see Figure 3-1). Unlike Model 12, the interpolation for Model 6 is performed on the data for the moduli, Poisson's ratio and thermal expansion coefficients. These interpolated values are then used to define the strain-stress coefficients given in Figure 2-2 and inverted to give the stress-strain law given in Figure 2-3.

The strain dependency is not based on an effective strain, because as described in Appendix C this would be a nontrivial computation for an anisotropic material. Instead the strain dependency is of the following form

$$
\begin{aligned}
E_a &= E_a(\varepsilon_a, T)\\
E_b &= E_b(\varepsilon_b, T)\\
E_c &= E_c(\varepsilon_c, T)\\
G_{ab} &= G_{ab}(\gamma_{ab}, T)\\
G_{ac} &= G_{ac}(\gamma_{ac}, T)\\
G_{bc} &= G_{bc}(\gamma_{bc}, T)\\
\nu_{ab} &= \nu_{ab}(T)\\
\nu_{ac} &= \nu_{ac}(T)\\
\nu_{bc} &= \nu_{bc}(T)\\
\alpha_a &= \alpha_a(T)\\
\alpha_b &= \alpha_b(T)\\
\alpha_c &= \alpha_c(T)
\end{aligned}
$$

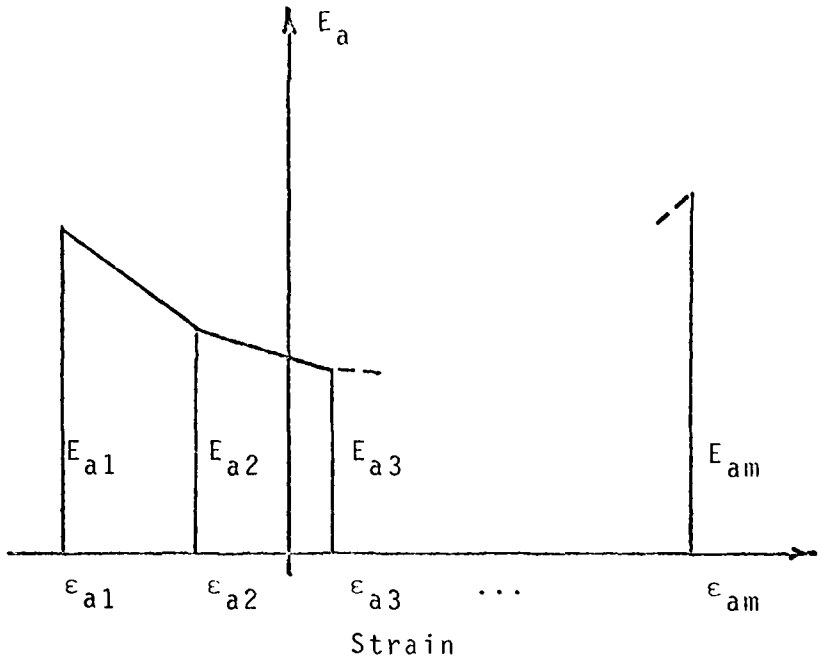

Figure 3-1. Model 6 Strain Interpolation Method.

This approach was chosen for several reasons. The moduli are usually measured in a uniaxial stress test and, thus, their strain dependency is primarily related to the uniaxial strain. Data for the strain dependency of Poisson's ratio is rarely available and when it is, it is usually not reliable. Varying the 3 Poisson's ratios can lead to numerical difficulties that may not be easy to identify. The temperature dependency of Poisson's ratio can likewise cause problems and should be avoided whenever possible (also the case for Model 12). However, variation of the uniaxial and shear moduli can be made over a large range without numerical problems. The coefficients of thermal expansion were taken to be independent of strain since virtually no data exists to identify this dependency.

A small number of modifications to the ADINA 78 User's Manual[3] are necessary in order to describe how to use Model 6. However, there are no changes for any other material models. Rather than reproducing extensive portions of the user's manual, in the sequel only the modifications and additions to the manual are described.

Modifications for the 2D and 3D Solid Element Input Data (MODEL 6)

Element Group Control Card

Columns	*Variable*	Entry
•		
•		
•		
45-48	K=NP AR(12)	Number of strain points (≥2, Model 6 only)
•		
•		
53-56	M=NP AR(14)	Number of temperature points (Models 6 & 12 only)
57-60	NP AR(15)=6	Material model number; 6 is the Orthotropic Thermoelastic Strain Dependent Model number.
•		
•		
•		

Set NP AR(15)=6 to activate the material Model 6 input data. K=NP AR(12) defines

the number of strain points at which material properties are to be defined, K ≥ 2 and is only used with Model 6. M=NPAR(14) defines the number of temperature points, for each strain point, for which material properties are to be input. NPAR(14) is used for both Model 6 and 12, but with Model 6 NPAR(15) can be given as 1 (0 is reset to 1) in order that strain dependent, temperature independent material properties can be defined.

	Columns	Variable	Entry
Card Set 1-1			
	1-10	PROP(1,N,1,1)	E_{a11} a-direction modulus at point 1,1
	11-20	PROP(2,N,1,1)	E_{a21} a-direction modulus at point 2,1
		•	•
		•	•
		•	•
		PROP(K,N,1,1)	E_{ak1} a-direction modulus at point k,1
Card Set 1-2			
	1-10	PROP(1,N,2,1)	E_{a12} a-direction modulus at point 1,2
	11-20	PROP(2,N,2,1)	E_{a22} a-direction modulus at point 2,2
		•	•
		•	•
		•	•
		PROP(K,N,2,1)	E_{ak2} a-direction modulus at point k,2
•			
•			
•			
Card Set 1-M			
	1-10	PROP(1,N,M,1)	E_{a1m} a-direction modulus at point 1,m
	11-20	PROP(2,N,M,1)	E_{a2m} a-direction modulus at point 2,m
		•	•
		•	•
		•	•
		PROP(K,N,M,1)	E_{akm} a-direction modulus at point k,m
Card Set 2-1			
	1-10	PROP(1,N,1,2)	ε_{a11} a-direction strain at point 1,1
	11-20	PROP(2,N,1,2)	ε_{a21} a-direction strain at point 2,1
		•	•
		•	•
		•	•
		PROP(K,N,1,2)	ε_{ak1} a-direction strain at point k,1

Card Set 2-2

1-10	PROP(1,N,2,2)	ε_{a12} a-direction strain at point 1,2
11-20	PROP(2,N,2,2)	ε_{a22} a-direction strain at point 2,2
	PROP(K,N,2,2)	ε_{ak2} a-direction strain at point k,2

Card Set 2-M

1-10	PROP(1,N,M,2)	ε_{a1m} a-direction strain at point 1,m
11-20	PROP(2,N,M,2)	ε_{a2m} a-direction strain at point 2,m
	PROP(K,N,M,2)	ε_{akm} a-direction strain at point k,m

Card Set 3-1

1-10	PROP(1,N,1,3)	E_{b11} b-direction modulus at point 1,1
11-20	PROP(2,N,1,3)	E_{b21} b-direction modulus at point 2,1
	PROP(K,N,1,3)	E_{bk1} b-direction modulus at point k,1

Card Set 3-M

1-10	PROP(1,N,M,3)	E_{b1m} b-direction modulus at point 1,m
11-20	PROP(2,N,M,3)	E_{b2m} b-direction modulus at point 2,m
	PROP(K,N,M,3)	E_{bkm} b-direction modulus at point k,m

Card Set 4-1

1-10	PROP(1,N,1,4)	ε_{b11} b-direction strain at point 1,1
11-20	PROP(2,N,1,4)	ε_{b21} b-direction strain at point 2,1
	PROP(K,N,1,4)	ε_{bk1} b-direction strain at point k,1

Card Set 4-M

1-10	PROP(1,N,M,4)	ε_{b1m} b-direction strain at point 1,m
11-20	PROP(2,N,M,4)	ε_{b2m} b-direction strain at point 2,m
	PROP(K,N,M,4)	ε_{bkm} b-direction strain at point k,m

Card Set 5-1

1-10	PROP(1,N,1,5)	E_{c11} c-direction modulus at point 1,1
11-20	PROP(2,N,1,5)	E_{c21} c-direction modulus at point 2,1
	.	.
	.	.
	.	.
	PROP(K,N,1,5)	E_{ck1} c-direction modulus at point k,1

.
.
.

Card Set 5-M

1-10	PROP(1,N,M,5)	E_{c1m} c-direction modulus at point 1,m
11-20	PROP(2,N,M,5)	E_{c2m} c-direction modulus at point 2,m
	.	.
	.	.
	.	.
	PROP(K,N,M,5)	E_{ckm} c-direction modulus at point k,m

Card Set 6-1

1-10	PROP(1,N,1,6)	ε_{c11} c-direction strain at point 1,1
11-20	PROP(2,N,1,6)	ε_{c21} c-direction strain at point 2,1
	.	.
	.	.
	.	.
	PROP(K,N,1,6)	ε_{ck1} c-direction strain at point k,1

.
.
.

Card Set 6-M

1-10	PROP(1,N,M,6)	ε_{c1m} c-direction strain at point 1,m
11-20	PROP(2,N,M,6)	ε_{c2m} c-direction strain at point 2,m
	.	.
	.	.
	.	.
	PROP(K,N,M,6)	ε_{ckm} c-direction strain at point k,m

Card Set 7-1

1-10	PROP(1,N,1,7)	G_{ab11} ab-shear modulus at point 1,1
11-20	PROP(2,N,1,7)	G_{ab21} ab-shear modulus at point 2,1
	.	.
	.	.
	.	.
	PROP(K,N,1,7)	G_{abk1} ab-shear modulus at point k,1

.
.
.

Card Set 7-M

1-10	PROP(1,N,M,7)	G_{ab1m} ab-shear modulus at point 1,m
11-20	PROP(2,N,M,7)	G_{ab2m} ab-shear modulus at point 2,m
	.	.
	.	.
	.	.
	PROP(K,N,M,7)	G_{abkm} ab-shear modulus at point k,m

Card Set 8-1		
1-10	PROP(1,N,1,8)	γ_{ab11} ab-shear strain at point 1,1
11-20	PROP(2,N,1,8)	γ_{ab21} ab-shear strain at point 2,1
	•	•
	•	•
	•	•
	PROP(K,N,1,8)	γ_{abk1} ab-shear strain at point k,1
•		
•		
•		
Card Set 8-M		
1-10	PROP(1,N,M,8)	γ_{ab1m} ab-shear strain at point 1,m
11-10	PROP(2,N,M,8)	γ_{ab2m} ab-shear strain at point 2,m
	•	•
	•	•
	•	•
	PROP(K,N,M,8)	γ_{abkm} ab-shear strain at point k,m
Card Set 9-1*		
1-10	PROP(1,N,1,9)	G_{ac11} ac-shear modulus at point 1,1
11-20	PROP(2,N,1,9)	G_{ac21} ac-shear modulus at point 2,1
	•	•
	•	•
	•	•
	PROP(K,N,1,9)	G_{ack1} ac-shear modulus at point k,1
•		
•		
•		
Card Set 9-M*		
1-10	PROP(1,N,M,9)	G_{ac1m} ac-shear modulus at point 1,m
11-20	PROP(2,N,M,9)	G_{ac2m} ac-shear modulus at point 2,m
	•	•
	•	•
	•	•
	PROP(K,N,M,9)	G_{ackm} ac-shear modulus at point k,m
Card Set 10-1*		
1-10	PROP(1,N,1,10)	γ_{ac11} ac-shear strain at point 1,1
11-20	PROP(2,N,1,10)	γ_{ac21} ac-shear strain at point 2,1
	•	•
	•	•
	•	•
	PROP(K,N,1,10)	γ_{ack1} ac-shear strain at point k,1
•		
•		
•		

*Card Sets 9, 10, 11 and 12 are omitted for 2D Solid Elements.

Card Set 10-M*		
1-10	PROP(1,N,M,10)	γ_{ac1m} ac-shear strain at point 1,m
11-20	PROP(2,N,M,10)	γ_{ac2m} ac-shear strain at point 2,m
.	.	.
.	.	.
.	.	.
	PROP(K,N,M,10)	γ_{ackm} ac-shear strain at point k,m
Card Set 11-1*		
1-10	PROP(1,N,1,11)	G_{bc11} bc-shear modulus at point 1,1
11-20	PROP(2,N,1,11)	G_{bc21} bc-shear modulus at point 2,1
.	.	.
.	.	.
.	.	.
	PROP(K,N,1,11)	G_{bck1} bc-shear modulus at point k,1
.		
.		
.		
Card Set 11-M*		
1-10	PROP(1,N,M,11)	G_{bc1m} bc-shear modulus at point 1,m
11-20	PROP(2,N,M,11)	G_{bc2m} bc-shear modulus at point 2,m
.	.	.
.	.	.
.	.	.
	PROP(K,N,M,11)	G_{bckm} bc-shear modulus at point k,m
Card Set 12-1*		
1-10	PROP(1,N,1,12)	γ_{bc11} bc-shear strain at point 1,1
11-20	PROP(2,N,1,12)	γ_{bc21} bc-shear strain at point 2,1
.	.	.
.	.	.
.	.	.
	PROP(K,N,1,12)	γ_{bck1} bc-shear strain at point k,1
.		
.		
.		
Card Set 12-M*		
1-10	PROP(1,N,M,12)	γ_{bc1m} bc-shear strain at point 1,m
11-20	PROP(2,N,M,12)	γ_{bc2m} bc-shear strain at point 2,m
.	.	.
.	.	.
.	.	.
	PROP(K,N,M,12)	γ_{bckm} bc-shear strain at point k,m
Card Set 13		
1-10	PROP(1,N,1,13)	T_1 temperature at point 1
11-20	PROP(1,N,2,13)	T_2 temperature at point 2
.	.	.
.	.	.
.	.	.
	PROP(1,N,M,13)	T_m temperature at point m

*Card Sets 9, 10, 11 and 12 are omitted for 2D Solid Elements.

Card Set 14		
1-10	PROP(1,N,1,14)	ν_{ab1} ab-Poisson's ratio at point 1
11-20	PROP(1,N,2,14)	ν_{ab2} ab-Poisson's ratio at point 2
.	.	.
.	.	.
.	.	.
	PROP(1,N,M,14)	ν_{abm} ab-Poisson's ratio at point m
Card Set 15		
1-10	PROP(1,N,1,15)	ν_{ac1} ac-Poisson's ratio at point 1
11-20	PROP(1,N,2,15)	ν_{ac2} ac-Poisson's ratio at point 2
.	.	.
.	.	.
.	.	.
	PROP(1,N,M,15)	ν_{acm} ac-Poisson's ratio at point m
Card Set 16		
1-10	PROP(1,N,1,16)	ν_{bc1} bc-Poisson's ratio at point 1
11-20	PROP(1,N,2,16)	ν_{bc2} bc-Poisson's ratio at point 2
.	.	.
.	.	.
.	.	.
	PROP(1,N,M,16)	ν_{bcm} bc-Poisson's ratio at point m
Card Set 17		
1-10	PROP(1,N,1,17)	α_{a1} a-direction expan. coef. at point 1
11-20	PROP(1,N,2,17)	α_{a2} a-direction expan. coef. at point 2
.	.	.
.	.	.
.	.	.
	PROP(1,N,M,17)	α_{am} a-direction expan. coef. at point m
Card Set 18		
1-10	PROP(1,N,1,18)	α_{b1} b-direction expan. coef. at point 1
11-20	PROP(1,N,2,18)	α_{b2} b-direction expan. coef. at point 2
.	.	.
.	.	.
.	.	.
	PROP(1,N,M,18)	α_{bm} b-direction expan. coef. at point m
Card Set 19		
1-10	PROP(1,N,1,19)	α_{c1} c-direction expan. coef. at point 1
11-20	PROP(1,N,2,19)	α_{c2} c-direction expan. coef. at point 2
.	.	.
.	.	.
.	.	.
	PROP(1,N,M,19)	α_{cm} c-direction expan. coef. at point m
Card Set 20		
1-10	PROP(1,N,1,20)	TREF reference stress free temperature

3.4 Sample Problems for Model 6

The geometries and boundary conditions of the 2D and 3D Model 6 sample problems are the same as the Model 12 sample problems shown in Figures 2-4 and 2-5 and described in Section 2.4. The 2D Model 6 problem corresponds to the file R2D5 in Appendix A and the 3D problem to file R3D5. The ADINA 78 data for the 2D and 3D Model 6 sample problems are given in Tables 3.1 and 3.2, respectively. Both the strain and temperature variations were used in the problems, and a very interesting feature of this data is that the strain range is a function of temperature. A total of 3 strain points (NPAR(12)) and 2 temperature points (NPAR(14)) were used. Table 3.3 summarizes the data used for the 2D & 3D problems.

Table 3.3 Material Properties for MODEL 6 Sample Problems

Temperature	$\varepsilon_{(a,b,c)}$	E_a	E_b	E_c	G_{ab}
0	-1	0	0	0	0
0	0	0	0	0	0
0	1	0	0	0	0
100	-1	10×10^6	0	20×10^6	1×10^6
100	0	10×10^6	16.46×10^6	20×10^6	1×10^6
100	1	10×10^6	0	20×10^6	1×10^6

In functional form the moduli vary as follows

$$E_a = 10 \times 10^6 \text{ psi } (T/100)$$
$$E_c = 2E_a$$
$$G_{ab} = .1\ E_a$$
$$G_{ac} = .2\ E_a$$
$$G_{bc} = .3\ E_a$$

The E_b (hoop) modulus varies with temperature and strain

$$E_b = 16.46 \times 10^6 \text{ psi } (T/100)\ f(\varepsilon_b, 1)$$

where

$$f(\varepsilon_b, T) = \begin{cases} 1 + \varepsilon_b(100/T) & , \quad \text{for } -T/100 \leq \varepsilon_b \leq 0 \\ 1 - \varepsilon_b(100/T) & , \quad \text{for } 0 \leq \varepsilon_b \leq T/100 \end{cases}$$

Note that both the ε_b strain range and functional dependence of f vary with temperature. The Poisson's ratios and thermal expansion coefficients are constant

$$\nu_{ab} = .1$$
$$\nu_{ac} = .2$$
$$\nu_{bc} = .3$$
$$\alpha_a = .01$$
$$\alpha_b = .02$$
$$\alpha_c = .03$$

The a, b and c directions again correspond to r, θ and x, respectively.

The problem was run using a stress free reference temperature TREF = 10, an initial temperature of zero (which does not affect the calculations), and a constant temperature time history T = 10. Thus, there are no thermal strains and

$$E_a = 1 \times 10^6 \text{ psi}$$
$$E_b = 1.646 \times 10^6 \text{ psi } f(\varepsilon_B)$$
$$E_c = 2 \times 10^6 \text{ psi}$$
$$G_{ab} = .1 \times 10^6 \text{ psi}$$
$$G_{ac} = .2 \times 10^6 \text{ psi}$$
$$G_{bc} = .3 \times 10^6 \text{ psi}$$

and

$$f(\varepsilon_b) = \begin{cases} 1 + 10\varepsilon_b & , \quad -.1 \leq \varepsilon_b \leq 0 \\ 1 - 10\varepsilon_b & , \quad 0 \leq \varepsilon_b \leq .1 \end{cases}$$

The problem was run 1 load and step required 2 iterations. The final computed radial displacement was

$$u_r = -.166$$

Thus,

$$\varepsilon_\theta = \varepsilon_b = u_r/20 = -8.3 \times 10^{-3}$$

and

$$f(\varepsilon_b = -.083) = .917$$

and

$$E_b = 1.509 \times 10^6 \text{ psi}$$

The problem is again one of plane strain ($\varepsilon_x = 0$) in which the in-plane stresses are statically determinant

$$\sigma_r = \sigma_a \cong 0$$

$$\sigma_\theta = \sigma_b = \frac{pR}{t} = 13333 \text{ psi}$$

The strain-stress law becomes

$$\begin{Bmatrix} \varepsilon_r \\ \varepsilon_\theta \\ 0 \end{Bmatrix} = \begin{bmatrix} 1 & -.1/1.509 & -.1 \\ -.1/1.509 & 1/1.509 & -.15 \\ -.1 & -.15 & 1/2 \end{bmatrix} \begin{Bmatrix} 0 \\ \sigma_\theta \\ \sigma_x = \sigma_c \end{Bmatrix} \times 10^{-6}$$

and solving for σ_x and ε_θ gives

$$\sigma_x = -4000 \text{ psi}$$
$$\varepsilon_\theta = 8.24 \times 10^{-3}$$

So after 2 iterations the solution has converged to an accuracy of approximately 1% for the hoop strain.

Table 3.1. 2D Model 6 Sample Problem - File R2D5 Appendix A.

```
2-D HOOP MODEL 6
    48100111          1     1     1          1.                  1
           2
           9                                 2



           1     2



      2     2
      1     2
            0.          0.          10.          10.
      2     2
            0.          1.          10.          1.
X     1     1     0     1     1     1     1                 20.25
X     4     1     0     0     1     1     1                 20.25          5.     5
X    44     1     0     0     1     1     1                 20.25          85.
X     6     1     0     0     1     1     1                 20.25          10.    5
X    46     1     1     0     1     1     1                 20.25          90.
X     2     1     0     1     1     1     1                 20.00
X     7     1     0     0     1     1     1                 20.00          10.    5
X    47     1     1     0     1     1     1                 20.00          90.
X     3     1     0     1     1     1     1                 19.75
X     5     1     0     0     1     1     1                 19.75          5.     5
X    45     1     0     0     1     1     1                 19.75          85.
X     8     1     0     0     1     1     1                 19.75          10.    5
X    48     1     1     0     1     1     1                 19.75          90.
                 1     1
      1                 1
     49
     2    9    1         1                                3         2    6
      1

        1.0E7       1.0E7       1.0E7

          -1.           0.          1.

           0.16463414.6             0.

          -1.           0.          1.

        2.0E7       2.0E7       2.0E7

          -1.           0.          1.

        1.0E6       1.0E6       1.0E6

          -1.           0.          1.
           0.         100.0
           .1           .1
           .2           .2
           .3           .3
          .01          .01
```

Table 3.1 (cont'd) 2D Model 6 Sample Problem - File R2D5 Appendix A.

```
        .02         .02
        .03         .03
        10.
     1     8     1     1     5       .087266463          1.0
     3     1     6     8     2     4     7     5
     9     8     1     1     5       .087266463          1.0
    43    41    46    48    42    44    47    45
     2     1     1     6     4
333.33333 333.33333         1.0                    5
     2     1    41    46    44
333.33333 333.33333          1.
     1     2         10.                  1
    48     2         10.
STOP
```

Table 3.2. 3D Model 6 Sample Problem - File R3D5 Appendix A.

```
HOOP STRAIN  -   3D      PLANE STRAIN      MODEL 6
    97100111          1     1     1        1.              1
           2
                 9                  2



           1     2



      2    2
      1    2
          0.          1.        10.        1.
      2    2
          0.          1.        10.        1.
X     1    0     0     1     1     1     1                   19.75
X     7    0     0     0     1     1     1                   19.75         5.     10
X    87    0     0     0     1     1     1                   19.75        85.
X    11    0     0     0     1     1     1                   19.75        10.     10
X    91    0     1     0     1     1     1                   19.75        90.
X     3    0     0     1     1     1     1                   20.00
X    13    0     0     0     1     1     1                   20.00        10.     10
X    93    0     1     0     1     1     1                   20.00        90.
X     5    0     0     1     1     1     1                   20.25
X     9    0     0     0     1     1     1                   20.25         5.     10
X    89    0     0     0     1     1     1                   20.25        85.
X    15    0     0     0     1     1     1                   20.25        10.     10
X    95    0     1     0     1     1     1                   20.25        90.
X     2    1     0     1     1     1     1       -1.0        19.75
X     8    1     0     0     1     1     1       -1.0        19.75         5.     10
X    88    1     0     0     1     1     1       -1.0        19.75        85.
X    12    1     0     0     1     1     1       -1.0        19.75        10.     10
X    92    1     1     0     1     1     1       -1.0        19.75        90.
X     4    1     0     1     1     1     1       -1.0        20.00
X    14    1     0     0     1     1     1       -1.0        20.00        10.     10
X    94    1     1     0     1     1     1       -1.0        20.00        90.
X     6    1     0     1     1     1     1       -1.0        20.25
X    10    1     0     0     1     1     1       -1.0        20.25         5.     10
X    90    1     0     0     1     1     1       -1.0        20.25        85.
X    16    1     0     0     1     1     1       -1.0        20.25        10.     10
X    96    1     1     0     1     1     1       -1.0        20.25        90.
     97    1     1     1     1     1     1
                 1     1
      1                1
     97
     3    9    1            16                      3         2    6           9
      1

        1.0E7       1.0E7       1.0E7

          -1.          0.          1.

           0.16460414.6            0.
```

Table 3.2 (cont'd) 3D Model 6 Sample Problem - File R3D5 Appendix A.

```
   -1.          0.          1.

2.0E7       2.0E7       2.0E7

   -1.          0.          1.

1.0E6       1.0E6       1.0E6

   -1.          0.          1.

2.0E6       2.0E6       2.0E6

   -1.          0.          1.

3.0E6       3.0E6       3.0E6

   -1.          0.          1.
    0.       100.0
    .1          .1
    .2          .2
    .3          .3
   .01         .01
   .02         .02
   .03         .03
    10.
 1   97    7   95
 1   97   17   95
 1   97   27   95
 1   97   37   95
 1   97   47   95
 1   97   57   95
 1   97   67   95
 1   97   77   95
 1   97   87   95
 1   16   16    1    1    1        10
16   15    5    6   12   11    1   2
 0    9    0   10    0    7    0   8   14   13    3    4    0
 2   16   16    1    1    2        10
26   25   15   16   22   21   11   12
 0   19    0   20    0   17    0   18   24   23   13   14    0
 3   16   16    1    1    3        10
36   35   25   26   32   31   21   22
 0   29    0   30    0   27    0   28   34   33   23   24    0
 4   16   16    1    1    4        10
46   45   35   36   42   41   31   32
 0   39    0   40    0   37    0   38   44   43   33   34    0
 5   16   16    1    1    5        10
56   55   45   46   52   51   41   42
 0   49    0   50    0   47    0   48   54   53   43   44    0
 6   16   16    1    1    6        10
66   65   55   56   62   61   51   52
 0   59    0   60    0   57    0   58   64   63   53   54    0
 7   16   16    1    1    7        10
76   75   65   66   72   71   61   62
 0   69    0   70    0   67    0   68   74   73   63   64    0
```

Table 3.2 (cont'd) 3D Model 6 Sample Problem - File R3D5 Appendix A.

```
    0    16    16     1     1     0          10
   86    95    75    76    82    81    71    72
    0    79     0    80     0    77     0    78    84    83    73    74     0
    9    16    16     1     1     9          10
   96    95    85    86    92    91    81    82
    0    89     0    90     0    87     0    88    94    93    83    84     0
    1    16    15     5     6     0     9     0    10
333.3333  333.3333  333.3333  333.3333                      10
    1    96    95    85    86     0    89     0    96
333.3333  333.3333  333.3333  333.3333
STOP
```

4. VECTORIZATION AND OPTIMIZATION OF ADINA ON THE ASC

4.1 General

The ASC is a unique fourth generation digital computer that is capable of executing single floating point operations at speeds comparable to typical third generation mainframe computers (e.g., CDC 6600). The mode of computation of single floating point operations, typically these floating point operations are intermixed with integer or logical operations, is called the scalar mode on the ASC. The ASC is also capable of performing vectorized floating point operations up to 20 times faster than scalar operations. The term vectorization on the ASC refers to the "pipeline" execution of the same sequence of floating point operations. The ASC has the capability of simultaneously performing multiple pipeline operations. Typically, the time required to initiate and/or terminate the pipeline process is approximately the same as the time to perform a single, scalar operation, i.e., about 20 clock cycles. However, once the pipeline is initiated, subsequent floating point operations require a single cycle. This very powerful feature of the ASC was expected to substantially improve the efficiency of ADINA, and a portion of the present effort was directed at vectorizing ADINA.

A second feature of the effort described in this section is optimization. On the ASC there are two compilers; a "fast" compiler that does little optimization of the assembler instructions, and a "slow" compiler that seeks to develop more efficient assembler code from the FORTRAN instructions. These two compilers are apparently similar to the OPT=1 and OPT=2 options on the standard CDC FTN compiler. Both the fast and slow compilers have 4 levels of optimization that can be selected. In most results reported herein, the default level 3 was used.

4.2 Vectorization Considerations

Vectorizable FORTRAN coding is typically in a tight DO loop of the following form

```
      DO  10  I= 1,1000
      A(I) = A(I)+B(I)* C(I)
10    CONTINUE
```

The major computational effort in the above loop is the floating point multiplication and addition. Such loops are commonly used to assess the computational efficiency of codes, and the effort in the above loop is rated at 1000 flops (floating point operations).[8] However, even a cursory inspection of the assembler code generated by the FORTRAN compiler will reveal that a significant number of overhead, nonvectorizable operations such as memory fetches, stores, integer addition and testing must also be performed. However, fourth generation computers such as the ASC, CRAY, STAR, etc. are capable of completing the 1000 passes through the loop substantially faster than 1000 arbitrary, scalar floating point operations.

In well written finite element code such as ADINA, the bulk of the CP (Central Processing) time is consumed in the formation of the element stiffness matrices and in the solution of the assembled simultaneous equations. Some processing time must also be spent performing Input/Output (I/O) tasks and other non-CP operations such as reading and writing to low speed disc storage. During the formation of the element matrices, a substantial number of computations similar to the above loop are performed. However, the range of these loops is typically small (8 integration points, 8 shape functions, 8 nodes, etc.) Thus, while many repetitive, similar calculations are made, their ranges are small. Vectorization is most efficient when many passes (100) are made through each loop. For this reason, the most important subroutine for vectorization is COLSOL[8,9], the column solver routine.

The word length on the ASC is 32 binary bits, the standard length for IBM look-alike computers. This length is marginally adequate for explicit, scalar floating point operations. However, at least 48 bits are required to retain sufficient accuracy for large implicit calculations such as those performed by ADINA. For this reason, all the floating point variables in ADINA were made double precision, 64 bits. This has some adverse effects on optimization and vectorization.

4.3 Benchmark Results

The important computations in a typical column[9] or frontal[8] type equation solver can be represented by the following nested loops

```
      TOT=0.0
      DO 20 N=1,1000
      SUM=0.0
      DO 10 I=1,10000
      SUM=SUM+A(I)*A(I+N)
10    CONTINUE
      TOT=TOT+SUM/10000.
20    CONTINUE
```

A loop structure of this type has been benchmarked on many different computers, and has been found to be a very good benchmark for purposes of comparing the computational efficiency of different computers. Since there are 10 million passes through the innermost loop, the computational effort is rated at 10 Mflops (Million floating point operations).

On the ASC the same loops were run using 3 compiler options: (1) using the fast compiler with the default level of "optimization" and no vectorization (vectorization cannot be performed with this compiler); (2) using the slow compiler with the default level of optimization and no vectorization; and (3) using the slow compiler with the default level of optimization but giving the compiler space to perform the vectorization. Although it is possible to modify the FORTRAN coding to make direct calls to vector processing routines, this was not done in any of the work reported herein.

Table 4.1 lists in ascending order the central processing (CP) time in seconds required to execute the 10 Mflop benchmark case. Unless specifically noted, the compilation was done using the best applicable level of optimization and the arithmetic was done using at least 60 binary bits. In some cases the comparable single precision time is also given.

The entries in Table 4.1 should be very carefully studied for they convey significant information about very important parameters. The vectorized Cray time is excellent, reflecting a computational speed of 15×10^6 floating point operations per second. However, scalar arithmetic on the Cray is noticably slower than the CDC 176 (same as a CDC 7600). The range of times in the table vary by a factor of almost 100.

Table 4.1. CP Run Times for 10 Mflop Benchmark

Computer	CP Time (Sec)	Remarks
Cray-1	.69	Vectorized
ASC	.82	Vectorized, Single Prec
ASC	3.2	Vectorized
CDC 176	4.1	
Cray-1	4.9	
UCS CDC 175	5.7	
SUN CDC 750	6.6	
CDC 176	7.2	No Opt (OPT=1)
BCS CDC 175	7.3	
ASC	16.	Slow Compiler, Default OPT
CDC 6600	20.	
ASC	26.	Slow Compiler, No OPT
UNIVAC 1100/80	34.	Single Prec
UNIVAC 1100/80	48.	
ASC	56.	Fast Compiler, Default OPT

The ASC is seen to be very fast for single precision arithmetic, but double precision increases the run time by a factor of 4. This is most unfortunate for ADINA (or any implicit code) since it cannot be run in single precision with accuracy. However, explicit codes such as finite difference or hydro-codes that can use single precision even for structural response calculations might run very efficiently on the ASC.

The importance of vectorization is also shown in the table. The slow compiler ran 5 times faster when vectorization was used. This is a big improvement but substantially less than the theoretical maximum factor of 20. Since the limit on the inner loop was 10,000, the overhead associated with pipeline initiation should be negligible. Thus, it would appear that the best vectorization the compiler can effect for double precision is a 5 fold reduction in run

time. Also, the 16 second run time with the slow (optimizing) compiler is barely faster than the CDC 6600. This implies that the scalar speed of the ASC in double precision is quite slow. The run time from the fast compiler seems incredibly slow, even slower than a UNIVAC. It is hard to understand a factor of 3.5 between the fast and slow computers on the ASC. On the CDC 176 the factor is less than 2.

ADINA Benchmark

While the loop structure accurately reflects the equation solver effort, the final evaluation must be of actual runs of ADINA. The table below lists the ASC and CDC 176 CP times for six 2D and six 3D runs. All of the ASC runs used the best optimized and vectorized version of ADINA that was developed during this effort.

Table 4.2 ASC vs. CDC ADINA Run Times (CP seconds)

	2D			3D		
	ASC	CDC176	Ratio	ASC	CDC176	Ratio
1	.81	.22	3.68	9.0	1.90	4.73
2	1.01	.23	4.39	8.86	2.01	4.40
3	1.14	.28	4.07	1.21	.37	3.27
4	4.58	.73	6.27	18.56	6.79	2.73
5	1.80	.39	4.61	10.62	2.25	4.72
6	13.97	1.89	7.59	53.81	9.16	5.87
Average			5.1	Average		4.3

The ASC is seen to run ADINA slower than the CDC 176, typically 4-5 times slower. In one 3D case the factor was less than 3, and the efficiency on the ASC seemed to improve as the problem size increased. The above problems are obviously small with run times not exceeding 1 minute on the ASC. The small size might bias the results unfavorably against the ASC.

Referring to Table 4.1, the CDC 176 was found to be approximately 4 times faster than the optimized ASC running in a scalar mode (no vectorization). The ratios in Table 4.2 suggest that the vectorization of ADINA may have had little effect on the run time. This suggestion is supported by the run times recorded compiling ADINA with the fast

compiler (these results have not been reported) which generally run only 2 times slower than with the best optimization and vectorization. Again referring back to Table 4.1, the fast compiler ran 3.5 times slower than the scalar mode of the optimizing compiler and 17.5 times slower than the best optimized and vectorized compiler. However, the 10 Mflop benchmark is strongly dominated by pipeline floating point operations, and in ADINA nearly 90% of the executable statements involve non-floating point or scalar floating point operations. Thus, it is not unreasonable that the run times with ADINA would be slower in relation to the CDC 176 (a very fast scalar computer) than the 10 Mflop benchmark or that the slow compiler would be less effective on ADINA than on the benchmark.

4.4 Discussion

The results of the vectorization and optimization studies presented in this section are surprising and disappointing. The best ASC double precison run of the 10 Mflop benchmark was 20% faster than a CDC 176, but the best ASC run times on ADINA are 4 times slower than the CDC 176. Without further, more detailed studies it is not possible to be certain about the cause of the ADINA inefficiency. However, the most likely cause is the very high percentage of scalar operations in ADINA and the very poor efficiency of the ASC in performing scalar computations. It is unlikely that further significant improvements can be made in ADINA using the current best (slow) compiler. If many large problems (30 minutes) are to be run, it would be worthwhile to force vectorization in the equation solver by modifying the FORTRAN. The bulk of ADINA should be left as is and future improvements in efficiency should be done using small subsets of the ADINA code, e.g., equation solver, assembler, element stiffness routines, etc.

At the start of this effort, we were told that the slow compiler was unreliable and often ran 5 times slower than the fast compiler. Our findings were that the slow compiler was quite reliable and that it typically ran 3 times slower. The CDC FTN OPT=2 compiler typically runs 2 times slower than OPT=1 and its object code typically runs 2 times faster. We found no reason to use the fast compiler and recommend that its use be discontinued.

The main reason that the ADINA run times are so slow is probably due to the compiler. The run times on the 10 Mflop benchmark varied from .8 to 56 seconds. This

is an unacceptable range. Reliable compilers that never take longer than 10 seconds in single precision should be provided. Also, it is surprising that scalar operations are so slow. Again, we suspect the compiler or operating system. Our opinion is that until basic improvements in the ASC are made, ADINA will continue to run 4 times slower than on a CDC 176.

5. CONCLUSIONS

The work reported herein has lead to significant improvements in the ADINA code on NRL's ASC computer. Material Model 12 was added to the 2D and 3D solid element types in order to permit the modeling of anisotropic thermoelastic materials, and material Model 6 was added to these same element types to permit the modeling of strain dependent nonlinear anisotropic thermoelastic materials. These additions should markedly improve NRL's ability to accurately determine the response of naval structures to intense rapid heating.

Considerable effort was also directed at improving the efficiency of ADINA on the ASC. Through use of optimization and vectorization, ADINA now runs at least twice as fast on the ASC. Unfortunately, ADINA still runs four times slower on the ASC than on a CDC 176. As discussed in Section 4, this is probably caused by the poor compiler provided by FTL. The current work did not attempt the solution of any large scale problems and it is likely that the ASC will improve its ratio to the CDC 176 on large problems. It is possible that by modifying the FORTRAN instructions in ADINA to make direct calls to assembler language vector processing routines, the run times can be further reduced. However, it is doubtful the ADINA will ever run faster on the ASC than on a CDC 176.

A great deal has been done to improve ADINA, but more remains to be done. The next Section 6 gives a detailed list of recommendations for further work in this area.

6. RECOMMENDATIONS

Much has been done to make ADINA operational and run efficiently on the ASC, but much remains to be done. The following is a list of recommended improvements and modifications to ADINA.

6.1 Development of a Preprocessor

ADINA has no preprocessing or data generation capabilities and its input structure is exceeding complex, occassionally redundant, and inconvenient to use. This condition detracts from effective utilization and wastes many hours of labor in the data preparation process. A preprocessor with some form of data generation should be developed as soon as possible. At a minimum this should include a free format reader and nodal point and element generator such as TEXGAP-2D[10] or TEXGAP-3D[11].

6.2 Development of a Postprocessor

The output from ADINA consists entirely of printed output, no graphical output is available. However, ADINA does have "portholes" that permit some user interaction with the code (for both pre and post processing). A postprocessing module should be developed to identify maximum and minimum stresses and strains by material and element group and to plot element connectivities, deformed grid, and stress and strain contours on parametric surfaces. This should be done using a "neutral plot file" concept such as used by Pacifica Technology in the TEXGAP codes.

6.3 Render all of ADINA 78 Operational on the ASC

At present only the 2D and 3D solid element types are operational for static and transient analyses. The other element types such as truss, beam, shell and fluid elements should be made operational and fully checked out. Several auxiliary options such as frequencies, creep, etc. also should be made operational.

6.4 Further Efficiency Improvement

A low level of effort as described in Section 4.4 should be continued in order to ascertain the most efficient method of running ADINA on the ASC.

6.5 Local Orthotropic Material Properties

Most of the anisotropic materials that are used in typical structures are transversely or locally orthotropic. The local orthotropic axes usually vary as, for example, with axisymmetric shells. The capability to model these locally orthotropic materials and variable local axes orientation should be added to ADINA to permit the more effective modeling of these materials.

6.6 Development of a New Shell Element

The shell element implemented in ADINA is suitable mainly for moderately thick shells and transitions from shell to solid (continuum) element types. This element is unsuitable for general shells and it is particularly inefficient for thin shells, a class of problems of considerable interest to the Navy. A new shell element should be developed and added to ADINA, retaining the current element as an option. A stiffener (beam) element that is compatible with the shell element should also be developed since many naval shell structures are stiffened.

6.7 Addition of Material Models to the Shell Element

Presently the shell element is limited to isotropic elastic or plastic material models. No thermoelastic or orthotropic materials can be modeled. The MODEL=2,3,6 & 12 material models should be added to the shell element.

6.8 ADINA-T Interface

NRL has put considerable effort into implementing and optimizing both ADINA and ADINA-T on the ASC. The interface between these codes should be thoroughly tested and upgraded to meet the needs of NRL.

6.9 Evaluation & Improvement of Nonlinear Algorithms

As described in Appendix B, there are open questions about the nonlinear solution algorithms used in ADINA. The code has been thoroughly checked out on linear static and dynamic and static nonlinear elastic problems. However, even highly skilled users have reported problems with ADINA most notably for dynamic plasticity problems. The present version of ADINA does not permit variable (adaptive) time steps. This is a serious deficiency that must be removed if dynamic nonlinear problems are to be run efficiently.

6.10 Improved Documentation

While the documentation of ADINA is voluminous, it is severely limited in scope, fails to give the user necessary guidance or recommendations, and is very difficult for the uninitiated to read and learn from. Personnel at the NRL and other Navy labs would be able to make much more effective and efficient use of the code if better documentation were available.

ADINA is coded in easy-to-read FORTRAN, and it is organized into modular, functional overlays that perform identifiable, logical tasks. Thus, ADINA is relatively easy to modify. For example, adding a new element type such as an improved shell element or adding new material models such as those described in Sections 2 and 3 can be done by a skilled programmer in a reasonable period of time. The personnel using ADINA could readily learn how to make these modifications themselves if a Programmer's Manual was available. A Programmer's Manual typically describes the organization of the code and the tasks performed by individual routines or groups of routines as well as describing the COMMON blocks, addressing and Input/Output structure. We recommend that such a document be prepared.

REFERENCES

[1] Bathe, K.-L., Ozdemire, H., and Wilson, E. L., "NONSAP-A Structural Analysis Program for Static and Dynamic Response of Nonlinear Systems," UC SESM Reports 74-3 & 4, University of California at Berkeley, February 1974.

[2] Bathe, K.-L., "ADINA - A Finite Element Program for Automatic Dynamic Incremental Nonlinear Analysis," Report 82448-1, M.I.T., September 1975.

[3] Bathe, K.-L., "ADINA - A Finite Element Program for Automatic Dynamic Incremental Nonlinear Analysis," Report 82448-1, M.I.T., Revised December 1978.

[4] Evans, R. J., "Constitutive Equations for a Class of Nonlinear Elastic Solids," UC SESM Report 65-5 and Ph.D. Dissertation, University of California at Berkeley, 1965.

[5] Evans, R. J., and Pister, K. S., "Constitutive Equations for a Class of Nonlinear Elastic Solids," Int. J. of Solids and Structures, 2/4, 1966.

[6] Weiler, F. C., "DOASIS - A Computer Code for the Deformation Plastic, Orthotropic, Axisymmetric (and Plane) Solution of Inelastic Solids," AFWL-TR-75-37, Vol. 1, October 1975.

[7] Jones, R. M. and Morgan, H. S., "Analysis of Nonlinear Stress-Strain Behavior of Fiber-Reinforced Composite Materials," AIAA, 15/12, December 1977.

[8] Dunham, R. S., "Evaluation of Out-of-Core Computer Programs for the Solution of Symmetric Banded Linear Equations," Pacifica Technology Report PT-U79-0330, December 1976.

[9] Bathe, K.-L., and Wilson, E. L., "Numerical Methods in Finite Element Analysis," Prentice Hall, 1976.

[10] Becker, E. B., and Dunham, R. S., "TEXGAP-2D User's Manual," AFRPL-TR-78-86, Vol I, February 1979.

[11] Becker, E. B., and Dunham, R. S., "TEXGAP-3D User's Manual," AFRPL-TR-78-87, Vol I, February 1979.

[12] Stricklin, J. A., Haisler, W. E., and von Riesmann, W., "Large Elastic-Plastic Response of Stiffened Shells of Revolution," ASME-74-PVP-3, 1974.

APPENDIX A
ADINA FILES ON THE ASC

This appendix describes the ADINA files that have been left on the ASC for future use. Any questions about these files should be directed to Dale Ranta at Pacifica Technology, 11696 Sorrento Valley Road, San Diego, California 92121, (714) 453-2530.

Path Name		USERCAT/D63/B80/DUNHRT
SONS:		
ADINA	-	Most of the ADINA files are on this path
MAC	-	MACROS
GET2D	-	MACRO to Get 2-D ADINA files from tape
GET3D	-	MACRO to Get 3-D ADINA files from tape
GETM	-	MACRO to Get 2-D/3-D ADINA files from tape
DAN	-	10 Mflops Benchmark problem

Path Name		USERCAT/D63/B80/DUNHRT/ADINA
Sons:		
NAMES	-	Names of ADINA files
AMAC	-	MACROS
LIBU	-	CIFER source librarys on this path
LIB	-	CIFER execution librarys on this path
ALINK	-	MARCO to link 2-D/3-D ADINA
ABS2D	-	Absolute element for 2-D ADINA
XQT2D	-	MARCO to execute 2-D ADINA
ABS3D	-	Absolute element for 3-D ADINA
XQT3D	-	MARCO to execute 3-D ADINA
LINK2D	-	MARCO to create ABS2D
LINK3D	-	MACRO to create ABS3D
SOURCE	-	Source code for MODEL 12
UP	-	MARCOS
UPDATE	-	CIFER update decks are on this path
RUNS	-	ADINA test problems are on this path
OUTPUT	-	ADINA test problem output is on this path

Path Name		USERCAT/D63/B80/DUNHR1/LIBU
SONS:		
ADINA	-	CIFER source for the "main" ADINA overlay
ADINT	-	CIFER source for the "input" ADINA overlay
EDDMTE	-	CIFER source for the "input" ADINA overlay
EDT2D3	-	CIFER source for the "input" ADINA overlay
EDT2D4	-	CIFER source for the "input" ADINA overlay
EDT2D6	-	CIFER source for the "input" ADINA overlay
EDT2D7	-	CIFER source for the "input" ADINA overlay
EDT2D8	-	CIFER source for the "input" ADINA overlay
ED2D10	-	CIFER source for the "input" ADINA overlay
ED2D12	-	CIFER source for the "input" ADINA overlay
ED2D13	-	CIFER source for the "input" ADINA overlay
ED2D14	-	CIFER source for the "input" ADINA overlay
THREDM	-	CIFER source for the "input" ADINA overlay
EDT3D3	-	CIFER source for the "input" ADINA overlay
EDT3D4	-	CIFER source for the "input" ADINA overlay
EDT3D6	-	CIFER source for the "input" ADINA overlay
EDT3D7	-	CIFER source for the "input" ADINA overlay
EDT3D8	-	CIFER source for the "input" ADINA overlay
ED3D10	-	CIFER source for the "input" ADINA overlay
ED3D12	-	CIFER source for the "input" ADINA overlay
DUMMY	-	CIFER source for the "input" ADINA overlay
BLOCK	-	CIFER source for the "input" ADINA overlay
LOAD	-	CIFER source for the "load" ADINA overlay

Path Name USERCAT/D63/B80/DUNHR1/LIB

SONS:

ADINA	-	CIFER execution library for the "main" ADINA overlay
ADINI	-	CIFER execution library for the "input" ADINA overlay
TODMFE	-	CIFER execution library for the "input" ADINA overlay
EDT2D3	-	CIFER execution library for the "input" ADINA overlay
EDT2D4	-	CIFER execution library for the "input" ADINA overlay
EDT2D6	-	CIFER execution library for the "input" ADINA overlay
EDT2D7	-	CIFER execution library for the "input" ADINA overlay
EDT2D8	-	CIFER execution library for the "input" ADINA overlay
ED2D10	-	CIFER execution library for the "input" ADINA overlay
ED2D12	-	CIFER execution library for the "input" ADINA overlay
ED2D13	-	CIFER execution library for the "input" ADINA overlay
ED2D14	-	CIFER execution library for the "input" ADINA overlay
THREDM	-	CIFER execution library for the "input" ADINA overlay
EDT3D3	-	CIFER execution library for the "input" ADINA overlay
EDT3D4	-	CIFER execution library for the "input" ADINA overlay
EDT3D6	-	CIFER execution library for the "input" ADINA overlay
EDT3D7	-	CIFER execution library for the "input" ADINA overlay
EDT3D8	-	CIFER execution library for the "input" ADINA overlay
ED3D10	-	CIFER execution library for the "input" ADINA overlay
ED3D12	-	CIFER execution library for the "input" ADINA overlay
DUMMY	-	CIFER execution library for the "input" ADINA overlay
BLOCK	-	CIFER execution library for the "input" ADINA overlay
LOAD	-	CIFER execution library for the "load" ADINA overlay

Path Name		USERCAT/D63/B80/DUNHR1/RUNS
SONS:		
R2D1	-	ADINA 2-D Test problem 1
R2D2	-	ADINA 2-D Test problem 2
R2D3*	-	ADINA 2-D Test problem 3
R2D4	-	ADINA 2-D Test problem 4
R2D5*	-	ADINA 2-D Test problem 5
R2D6	-	ADINA 2-D Test problem 6
R3D1	-	ADINA 3-D Test problem 1
R3D2*	-	ADINA 3-D Test problem 2
R3D3	-	ADINA 3-D Test problem 3
R3D4	-	ADINA 3-D Test problem 4
R3D5*	-	ADINA 3-D Test problem 5
R3D6	-	ADINA 3-D Test problem 6

*Sample problems described in Sections 2 and 3.

APPENDIX B
EXECUTION PROBLEMS

Personnel at Pacifica Technology have been using the ADINA code since its first release in 1975. While we have found it to be a very reliable code that solves a very large class of problems, we have also observed various execution errors. Almost all the difficulties we have noted are associated with the plasticity models and to a lesser degree, the constant time step.* This is especially true for plasticity problems with very rapid loading. ADINA almost always fails on this type of problem, except when the time step size is severely reduced (usually less than the Courant stability limit $\Delta t < \Delta x/c$).

Figures B-1 and B-2 illustrate a typical dynamic plasticity problem that ADINA has been unable to solve. An excellent numerical solution to this problem was computed with the DYNAPLAS code,[13] and recently a solution was also achieved with the STAGS-C1 code (this geometry was also used in an experiment reported by Wu and Witmer). Our ADINA run used a 5 μsec time step (certainly too large for good accuracy) and at the end of the first time step in the element at the crown the stress was ~67,000 psi and the radial displacement was ~.023". Thus, the strain from the strain displacement equations was $\varepsilon = u/r \sim .008$, but from the stress-strain law the plastic strain was $\varepsilon_p \sim (67{,}000 - 42{,}800)/.787 \times 10^5 \sim .32$, about 40 times the strain consistent with the displacements. In our opinion, this error is caused by a lack of closure in the plasticity routines, that is, a failure to test the stress state against the computed strain state.

These difficulties are potentially serious and warrant further investigation. However, NRL is not presently using ADINA for this type of problem. It is possible that this deficiency can be easily fixed, but this will not be known until a cure is attempted.

* It is remarkable that Bathe has been able to retain the constant time step in a general purpose nonlinear code.

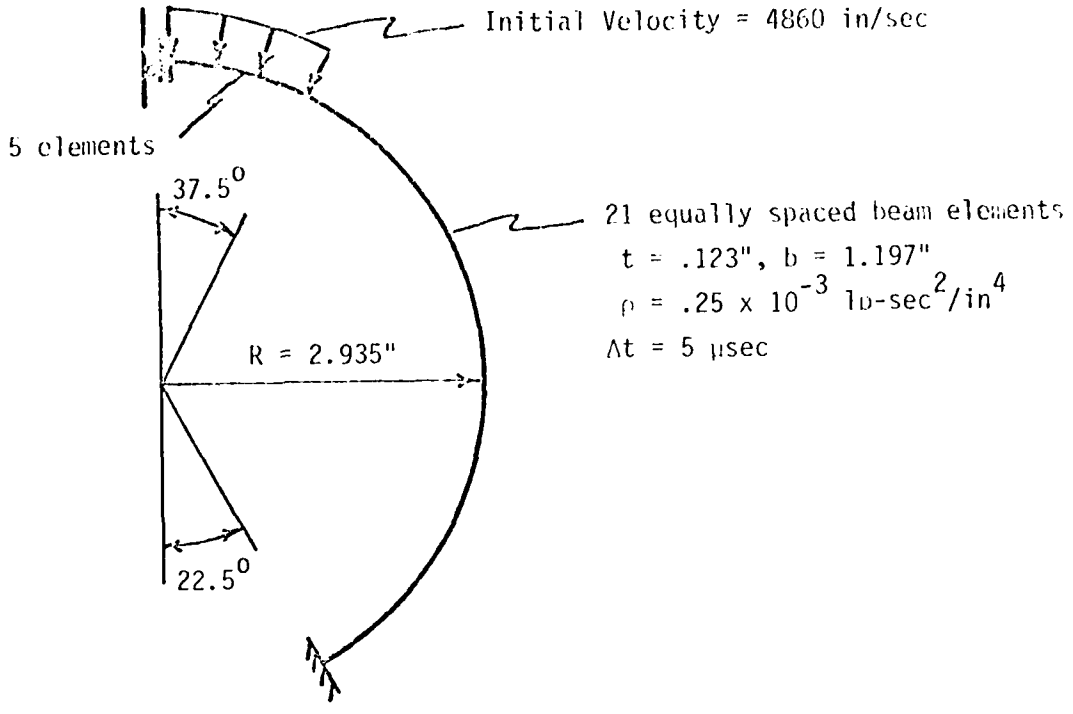

Figure B-1. Typical Dynamic Plasticity Problem for ADINA.

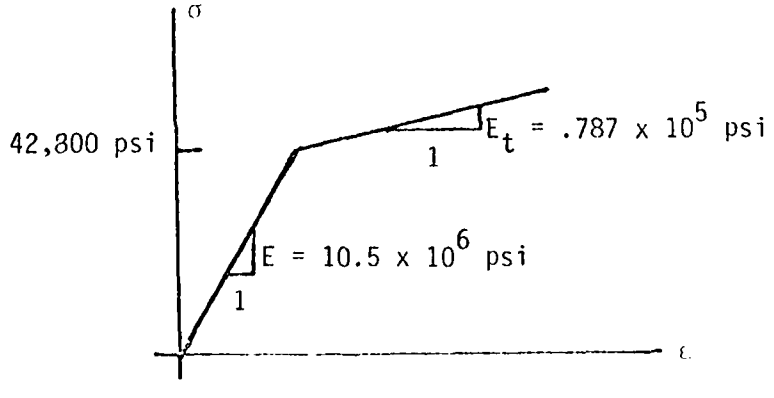

Figure B-2. Stress-Strain Law for Plasticity Problem.

APPENDIX C

ANISOTROPIC DEFORMATION THEORY PLASTICITY

Deformation Theory Plasticity is a theory that approximates the nonlinear stress-strain relationships of plasticity, but avoids the complexity of solving the actual plasticity equations. Within reasonable limits, this is generally a good approximation of material nonlinearity for loading histories without unloading and where the ratio of the stress components do not significantly change. Deformation theory gives results that are path independent and the theory is implemented using a secant modulus. Deformation theory can be readily incorporated into the ADINA computer code because although ADINA performs "incremental" solutions, it uses a secant modulus stiffness matrix for the Model 3 and the recently developed Model 12 temperature dependent properties, and the results are likewise load path independent.

The following development is for anisotropic deformation theory plasticity and illustrates how it could be incorporated into ADINA in a manner similar to Model 6. Isotropic materials would follow in a similar manner, and note that while the material is elastically isotropic, the secant (or tangent) stress-strain relationship becomes anisotropic after yield.

Anisotropic Stress-Strain Law

Derivations are limited to anisotropic materials that have stress-strain laws in the elastic range that are expressed in the principal material axes as

$$\{\sigma\} = [C^e]\ \{\varepsilon - \alpha\Delta T\} \qquad \text{(C-1)}$$

where

$$\begin{Bmatrix} \sigma_x \\ \sigma_y \\ \sigma_z \\ \tau_{xy} \\ \tau_{yz} \\ \tau_{zx} \end{Bmatrix} = \begin{bmatrix} C_{11} & C_{12} & C_{13} & 0 & 0 & 0 \\ C_{12} & C_{22} & C_{23} & 0 & 0 & 0 \\ C_{13} & C_{23} & C_{33} & 0 & 0 & 0 \\ 0 & 0 & 0 & C_{44} & 0 & 0 \\ 0 & 0 & 0 & 0 & C_{55} & 0 \\ 0 & 0 & 0 & 0 & 0 & C_{66} \end{bmatrix} \begin{Bmatrix} \varepsilon_x - \alpha_x\Delta T \\ \varepsilon_y - \alpha_y\Delta T \\ \varepsilon_z - \alpha_z\Delta T \\ \gamma_{xy} - \alpha_{xy}\Delta T \\ \gamma_{yz} - \alpha_{yz}\Delta T \\ \gamma_{zx} - \alpha_{zx}\Delta T \end{Bmatrix}$$

Figures C1a-C1f illustrate the uniaxial (stress) stress-strain behavior of the material in the principal material directions. For simplicity attention is limited to materials that have a linear hardening law. To fully describe a deformation theory anisotropic material it is necessary to measure 9 elastic moduli C_{11}, C_{12}, C_{13}, C_{22}, C_{23}, C_{33}, C_{44}, C_{55}, C_{66} (or equivalently the 9 engineering elastic properties E_x, E_y, E_z, ν_{xy}, ν_{yz}, ν_{zx}, G_{xy}, G_{yz}, G_{zx}), 6 coefficients of thermal expansion α_x, α_y, α_z, α_{xy}, α_{yz}, α_{zx}, 6 yield stresses Y_x, Y_y, Y_z, Y_{xy}, Y_{yz}, Y_{zx}, and 6 hardening moduli H_x, H_y, H_z, H_{xy}, H_{yz}, H_{zx}. Thus, there are 27 material properties to be measured. Also, all 27 of these material properties can be temperature dependent (the 9 elastic moduli and 6 coefficients of thermal expansion are functions of temperature in Model 12).

Anisotropic Effective Stress

Following closely Frank Weiler's development of the anisotropic deformation theory in the DOASIS code,[6] the existence of an effective stress measure (or equivalently an anisotropic yield function) in the following form is postulated

$$\bar{\sigma}^2 = \beta_1\left(\frac{\sigma_x}{r_x} - \frac{\sigma_y}{r_y}\right)^2 + \beta_2\left(\frac{\sigma_y}{r_y} - \frac{\sigma_z}{r_z}\right)^2 + \beta_3\left(\frac{\sigma_z}{r_z} - \frac{\sigma_x}{r_z}\right)^2 + \beta_{xy}\tau_{xy}^2 + \beta_{yz}\tau_{yz}^2 + \beta_{zx}\tau_{zx}^2 \qquad \text{(C-2)}$$

where the r weighting factors are chosen to make the effective stress independent of volumetric strains, thus, making the effective stress a measure only of deformation producing strain states.

$$r_x = (C_{11} + C_{12} + C_{13})/C,\ r_y=(C_{12} + C_{22} + C_{23})/C,\ r_z=(C_{13} + C_{23} + C_{33})/C \qquad \text{(C-3)}$$

where for convenience we choose $C = C_{11} + C_{12} + C_{13}$ and, thus, $r_x = 1$. Now define

$$\begin{aligned} \beta_x &= \beta_1 + \beta_3 \\ \beta_y &= \beta_1 + \beta_2 \\ \beta_z &= \beta_2 + \beta_3 \end{aligned} \qquad \text{(C-4a)}$$

and the inverse relations

$$\beta_1 = \frac{1}{2}\ (\beta_x + \beta_y - \beta_z)$$
$$\beta_2 = \frac{1}{2}\ (-\beta_x + \beta_y + \beta_z) \qquad \text{(C-4b)}$$
$$\beta_3 = \frac{1}{2}\ (\beta_x - \beta_y + \beta_z)$$

Also define

$$\frac{1}{\kappa_x} = \frac{1}{H_x} - \frac{1}{E_x}\ ,\quad \frac{1}{\kappa_y} = \frac{1}{H_y} - \frac{1}{E_y}$$
$$\frac{1}{\kappa_z} = \frac{1}{H_z} - \frac{1}{E_z}\ ,\quad \frac{1}{\kappa_{xy}} = \frac{1}{H_{xy}} - \frac{1}{G_{xy}} \qquad \text{(C-5)}$$
$$\frac{1}{\kappa_{yz}} = \frac{1}{H_{yz}} - \frac{1}{G_{yz}}\ ,\quad \frac{1}{\kappa_{zx}} = \frac{1}{H_{zx}} - \frac{1}{G_{zx}}$$

Anisotropic Effective Stress-Strain Relation

Next an anisotropic effective stress-strain relationship that is the same form as the uniaxial components is postulated. This is illustrated in Figure C2. The effective yield stress is $\bar{Y}$, The elastic modulus, $\bar{E}$, The hardening modulus is $\bar{H}$ and

$$\frac{1}{\bar{\kappa}} = \frac{1}{\bar{H}} - \frac{1}{\bar{E}} \qquad \text{(C-6)}$$

For convenience the effective stress-strain relation is chosen to be the same as the uniaxial $\sigma_x - \varepsilon_x$ relation, thus $\bar{Y} = Y_x$, $\bar{E} = E_x$, $\bar{H} = H_x$ and $\bar{\kappa} = \kappa_x$. This is arbitrary because the effective relation must embody all the component relations.

The β's are determined by equating the plastic work of each component to the plastic work of the effective stress. Without reproducing the algebraic details, this gives

$$\beta_i = \frac{r_i^2}{\dfrac{\kappa_i}{\bar{\kappa}} + \dfrac{Y_i^2 - \dfrac{\kappa_i}{\bar{\kappa}}\bar{Y}^2}{\bar{\sigma}^2}} \qquad \text{for} \quad i = x, y, z, xy, yx, zx \qquad \text{(C-7)}$$

Thus, we have the rather unpleasant result that the β's depend on the effective stress for an anisotropic material. (The β's are constants for an isotropic material.) Note that β_x=1 because of how we chose the normalizing factor for the r's and the effective stress-

strain relation.

Anisotropic Deformation Theory Flow Rule

Again omitting some algebraic details, the total plastic strain components are expressed

$$\varepsilon_i^p = \lambda S_i = \frac{\bar{\varepsilon}^p}{\bar{\sigma}} S_i \quad , \qquad i = x, y, z, xy, yz, zx \tag{C-8}$$

where λ is a positive proportionality factor, $\bar{\varepsilon}^p$ is the total effective plastic strain and S_i are the so-called anisotropic deviatoric stresses

$$S_i = \frac{1}{2} \frac{\partial \bar{\sigma}^2}{\partial \sigma_i} = B_{ij} \sigma_j \tag{C-9}$$

and

$$B_{ij} = \begin{bmatrix} \frac{\beta_x}{r_x r_x} & -\frac{\beta_1}{r_x r_y} & -\frac{\beta_3}{r_x r_z} & 0 & 0 & 0 \\ -\frac{\beta_1}{r_x r_y} & \frac{\beta_y}{r_y r_y} & -\frac{\beta_2}{r_y r_z} & 0 & 0 & 0 \\ -\frac{\beta_3}{r_x r_z} & -\frac{\beta_2}{r_y r_z} & \frac{\beta_z}{r_z r_z} & 0 & 0 & 0 \\ 0 & 0 & 0 & \beta_{xy} & 0 & 0 \\ 0 & 0 & 0 & 0 & \beta_{yz} & 0 \\ 0 & 0 & 0 & 0 & 0 & \beta_{zx} \end{bmatrix}$$

Also,

$$\bar{\varepsilon}^p = (\bar{\sigma} - \bar{Y})/\bar{\kappa} \quad , \tag{C-10}$$

and

$$\lambda = \frac{(\bar{\sigma} + \bar{Y})}{(\bar{\sigma}^2 + \bar{Y}^2)} \bar{\varepsilon}^p \tag{C-11}$$

Effective Secant Anisotropic Deformation Theory Stress-Strain Relation

The secant stress-strain law for the anisotropic deformation theory plasticity is expressed

$$\{\sigma\} = [C^{ep}] \{\varepsilon - \alpha \Delta T\} \tag{C-12a}$$

where

$$[C^{ep}] = [[D^e] + \lambda[B]]^{-1} \tag{C-12b}$$

and

$$[D^e] = [C^e]^{-1} \tag{C-12c}$$

[B] is the anisotropic deviatoric stress matrix given in (C-9) and $[C^e]$ is the elastic stress-strain matrix given in (C-1).

Implementation of the Anisotropic Deformation Theory

The following algorithm describes an iterative procedure by which the anisotropic deformation theory could be implemented into a code like ADINA. There are many alternatives that are simplier, but the method described below appears to be the most straightforward.

1) Using the current value of the secant modulus, $[C^{ep}]$, solve for the new total displacements in the next load or time step, $[C^{ep}] = [C^e]$ for $\bar{e}^p = 0$;
2) Using a Newton-Raphson iterative method compute the new effective stress, $\bar{\sigma}$, using equations (C-2)-(C-7);
3) Calculate the new estimate of the components of the plastic strain $\bar{\varepsilon}^p_i$ using either an explicit total strain or an explicit total work method (not described herein);
4) Calculate S_i, r_i, B_{ij}, λ and the total plastic strain components from (C-8) and the total stresses from (C-2a);
5) Repeat steps (2)-(5) until convergence is achieved for $\bar{\sigma}_i$ and $\bar{\varepsilon}^p_i$.

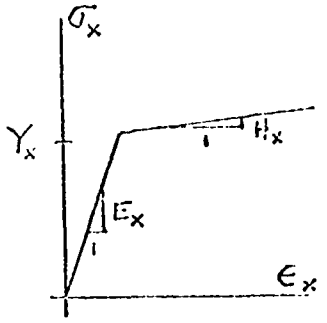

Figure C-1a

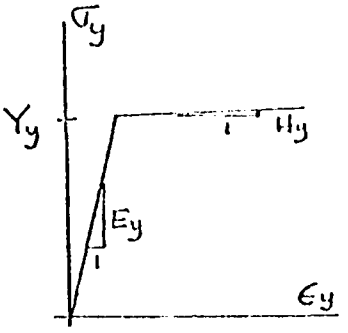

Figure C-1b

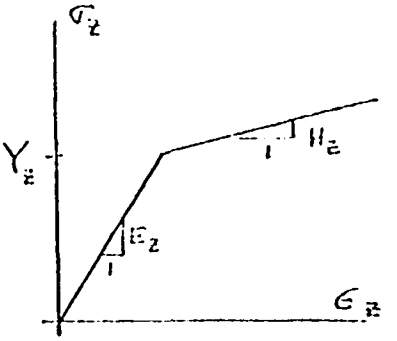

Figure C-1c

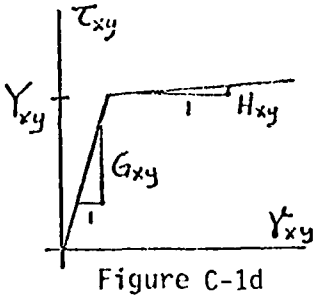

Figure C-1d

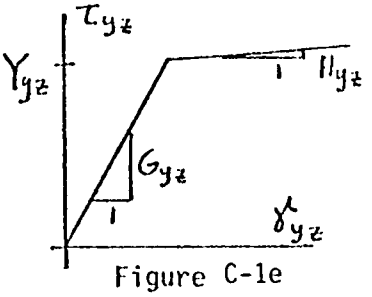

Figure C-1e

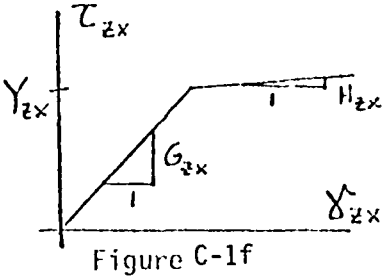

Figure C-1f

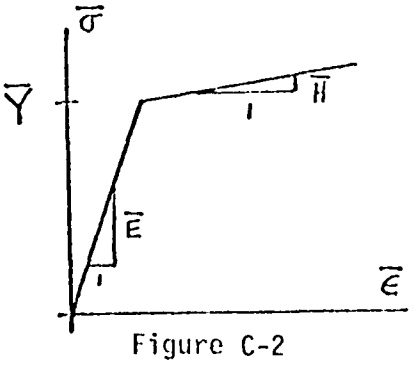

Figure C-2

DISTRIBUTION LIST

Department of the Navy

Naval Research Laboratory

ATTN: Code 2627, (6)

ATTN: Scientific Officer, (24)

Other Government Agencies

DCASMA San Diego, (1)

Defense Technical Information Center, (12)

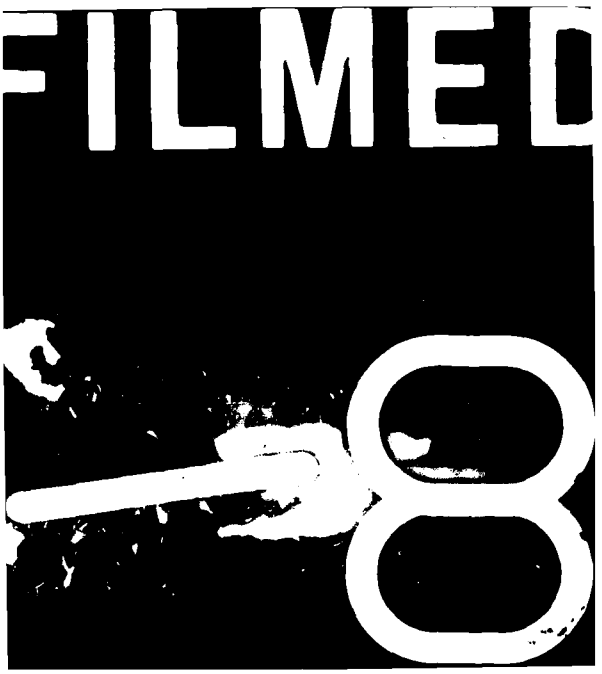
FILMED